Chapter 5

Base-mediated Tandem Intramolecular Amidation and Sulfenylation: Direct Access to 3-sulfenylated Imidazo[1,2-*a*]pyridin-2-ols

5.1 INTRODUCTION

The sulfur heterocycles and sulfur-derived functional groups constitute an integral part of numerous potential pharmaceuticals, agrochemicals, and materials.[1-3] The thioethers and their derivatives are regarded as important auxiliary units in numerous naturally occurring and bioactive compounds. Moreover, several structural scaffolds having aryl sulfide unit in their core structure have been used to treat different diseases such as cancer, Alzheimer's, HIV and malaria.[4-5] Some of the representative examples of C-S containing important molecules are depicted in **Figure 5.1**.

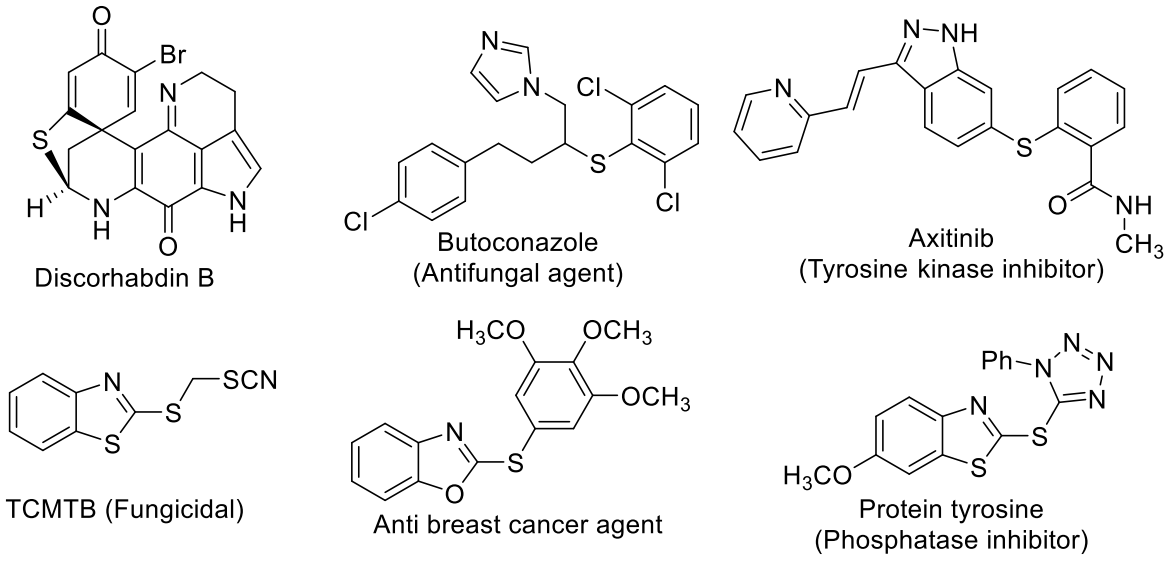

Figure 5.1 Representative examples of medicinally important thioether containing compounds

In light of the profuse importance of the sulfur containing compounds, the C-S bond formation reaction has sparked significant research efforts among synthetic chemists.[6-8] The C-S bond formation has been accomplished using various sulfenylating agents such as sulfites, sulfonyl chlorides, sulfonyl hydrazines or *S*-phenyl benzenesulfonothioate, disulfides and dithiocarbamates under either catalyzed by transition-metals or metal-free conditions or *via* uncatalyzed conditions.[9-13] The restrictions associated with the methods that use functionalized sulfenylating agents, transition-metal, excess reagents, and harsh reaction conditions allow looking into newer perspective to construct C-S bond in environmentally benign methods.

5.1.1 Cross-Dehydrogenative Coupling Reaction

In modern synthetic chemistry era, the cross-dehydrogenative coupling reactions (CDC) has emerged as an attractive tool for the construction of C-C, C-heteroatoms and heteroatom-heteroatom bonds. These reactions are regarded as highly atom-economical, environmentally benign and step economical in comparison to the traditional coupling reactions due to the elimination of the use of pre-functionalized starting materials and the byproduct of the reaction are two hydrogen atoms or water molecule with molecular oxygen used as the terminal oxidant.[14-16] Initially, the CDC approaches were carried out extensively using the complexes and salts of a transition-metal such as [Rh], [Ru], [Ir], [Cu], [Fe] or [Ni], with more emphasis given to palladium complexes because of its varied utilities.[17-18] However, cost-effectiveness, presence of transition metal impurity in the final product and generation of metallic waste products generally seizes the greener perspective of the strategy and limits the large scale practical applicability of transition-metal-mediated CDC reactions. In this particular aspect, transition metal-free C–C and C–heteroatom bond forming CDC reactions have witnessed important progress in recent years and there is no dearth of opportunities in the synthetic chemist's arsenal.[19] The transition metal-free reactions have represented a paradigm shift and the synthetic community has witnessed an unprecedented advancement in the field of cross-dehydrogenative coupling reactions.

5.1.2 Transition Metal-free C(sp^3)-S Bond Formation *via* Cross-Dehydrogenative Coupling Reactions

In spite of reaching great advances, the vast majority of the C–heteroatom bond forming CDC strategy is mostly confined to the construction of C-N and C-O bonds with only a few examples of C-S bond formations.[20] Generally, thiols are unstable under oxidative conditions as well as they are prone to bind with and quench the reactivity of metal complexes.[21] Consequently, the transition-metal-free direct cross-dehydrogenative coupling (CDC) reactions between C(sp^2)-H or C(sp^3)-H containing compounds and thiols have emerged as a powerful and alternate strategy for the formation of thioether bonds. In particular, the cross-dehydrogenative coupling reactions of thiols and active methylene compounds have generated much attention because this strategy represents a straightforward, efficient, and atom-economic process to access thioethers.

Yadav *et al*. reported direct sulfenylation of ketones (**2**) with thiols (**1**) using *N*-chlorosuccinimide (NCS) as an active reagent to produce α-ketothioethers (**3**) in excellent yield in DCM as solvent at room temperature. Different cyclic ketones like cyclopentanone, dodecanone, α-tetralone, α-tetralone and 4-phenylcyclohexanone along with aliphatic ketones were reacted well under optimized reaction condition. It was believed that *in situ* thiol converted to sulfenyl chloride in the presence of NCS which on nucleophilic substitution reaction with ketones furnished α-ketothioethers (**3**) (**Scheme 5.1**).[22]

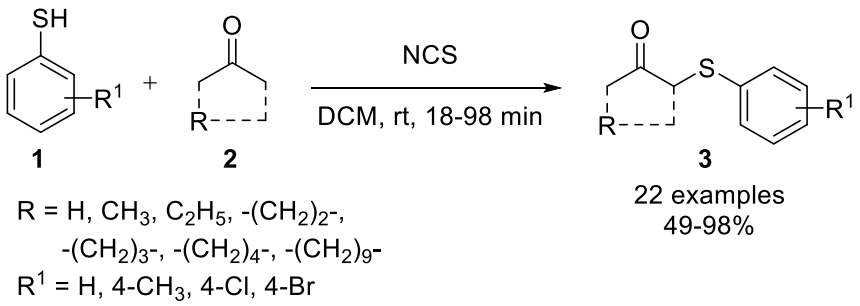

Scheme 5.1 *N*-Chlorosuccinimide-promoted synthesis of *a*-ketothioethers

Prabhu and coworkers developed the $K_2S_2O_8$-mediated cross-dehydrogenative sulfenylation of active methylene group of 1,3-diketones from the reaction of benzoxazole-2-thiones (**4**) and diketone derivatives (**5**) in the presence of aq. $HClO_4$ in acetonitrile at room temperature. In presence of base benzoxazole-2-thiones (**4**) converted to thiols which further in presence of $K_2S_2O_8$ and aq. $HClO_4$ was converted to benzoxazole-2-thio radicals *via* a single electron transfer (SET) mechanism. It was presumed that the benzoxazole-2-thio radical converted to either benzoxazole-2-thio persulfate intermediate or to disulphide intermediate and reacted with enol form of 1,3-diketones to furnish sulfenylated products. The sulfenyaltion of diketones without deacylation under metal-free condition was added advantage of this protocol (**Scheme 5.2a**).[23] The same synthetic strategy was also extended for the sulfenylation of methylketones (**7**). The optimized reaction condition was well tolerated by aliphatic and aromatic ketones. The broad substrate scope and ambient reaction conditions made the protocol advantageous (**Scheme 5.2b**).[24]

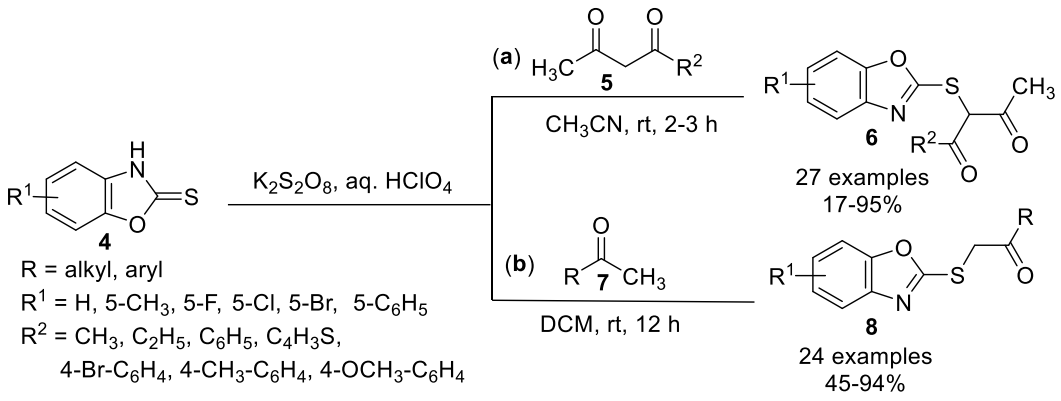

Scheme 5.2 $K_2S_2O_8$-mediated sulfenylation of 1,3-diketones/ ketones

Prabhu and coworkers also reported the iodine-mediated cross-dehydrogenative cross coupling reaction of heterocyclic thiones (**9**)/ thiols (**10**) with methyl ketone (**11**) using DMSO as oxidant as well as solvent. It was the first report for regioselective sulfenylation of methyl ketones in the presence of α-CH_2 or α-CH groups and aldehyde functionality (**Scheme 5.3**).[25]

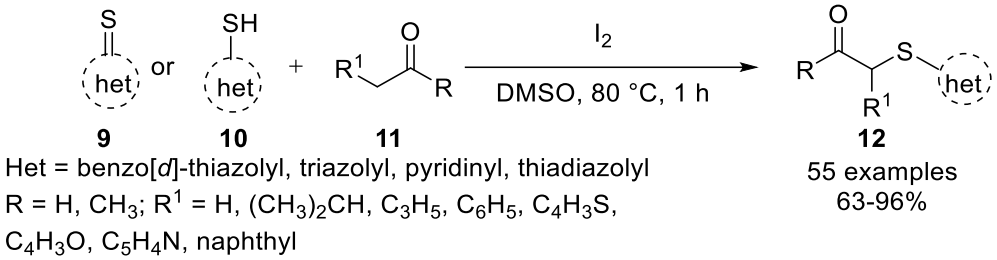

Scheme 5.3 I_2-mediated CDC reaction of heterocyclic thiones/thiols with ketones

Recently, the group developed a highly regioselective cross-dehydrogenative C(sp^3)-H sulfenylation of α-CH_3 or α-CH_2 bonds adjacent to α,β-unsaturated ketones (**13**) using dimethyl sulfoxide as an oxidant and a sub stoichiometric amount of aq. HI acid as an additive. The protocol exhibited a broad substrate scope of α,β-unsaturated ketones (**13**) with heterocyclic thiols (**10**) and produced sulfenylated products with a high regioselectivity without conjugate addition (**Scheme 5.4**).[26]

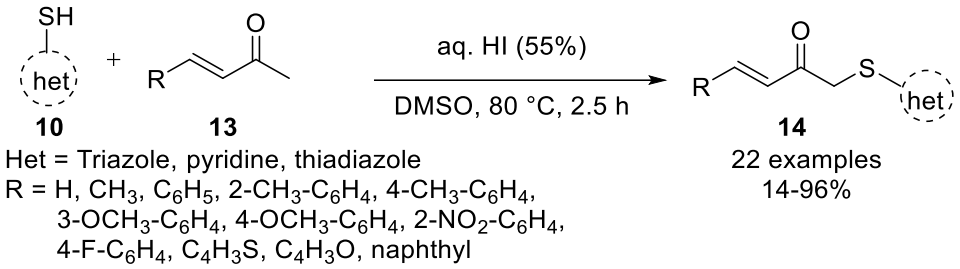

Scheme 5.4 The sulfenyltion of α,β-unsaturated ketones with heterocyclic thiols

The iodine-catalyzed oxidative coupling between 1,3-diketones (**5**) and thiophenols (1) to form β-dicarbonyl thioethers (**15**) was developed by Lei and co-workers. The reaction was performed in presence of catalytic amount of iodine and di-*tert*-butyl peroxide (DTBP) as oxidant under inert condition. The reaction was assumed to undergo through a radical substitution pathway instead of the usual nucleophilic substitution one (**Scheme 5.5** (**a**)).[27] Chen *et al*. reported the Cs_2CO_3-mediated cross-dehydrogenative coupling reaction of thiol (**1**) and active methylene compounds (**5**) under air as the terminal oxidant. The reaction included the formation of sulfide radical which eventually converted to disulfide which on the nucleophilic attack by the *in situ* generated enolate from methylene compounds afforded α-sulfenylated carbonyl compounds. The method was described as an efficient and environmentally friendly choice over existing methods (**Scheme 5.5** (**b**)).[28]

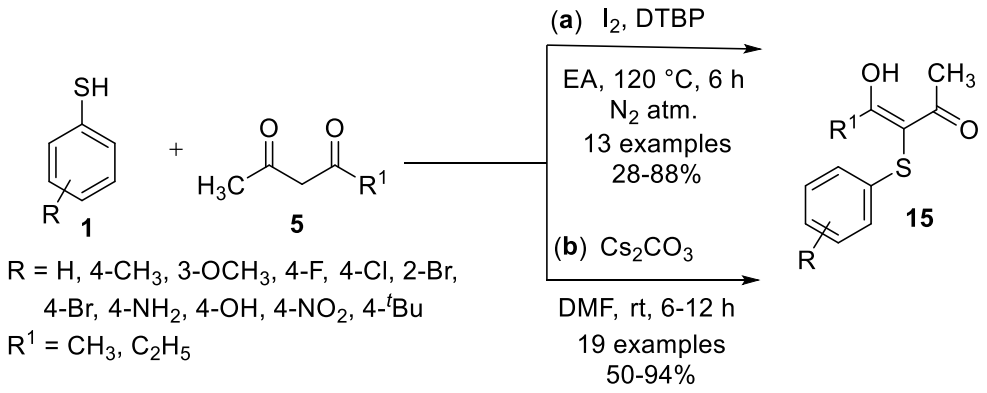

Scheme 5.5 (a) Iodine-catalyzed, and (b) Cs_2CO_3-mediated synthesis of β-dicarbonyl thioethers

Wang and co-workers constructed the sulfenylated pyrazoles *via* NaOH-mediated sulfenylation of pyrazolone and aryl thiols using acetonitrile as solvent (**Scheme 5.6** (**a**)).[29] Kamani *et al*. reported the sulfenyaltion of pyrazolone through N-chlorosuccinimide (NCS)-promoted direct

sulfenylation using aryl thiols at room temperature (**Scheme 5.6** (**b**)).[30] Prabhu and group synthesized the sulfenylated pyrazoles through iodine-catalyzed cross-dehydrogenative coupling of pyarazolones and diverse range of heterocyclic thiols and heterocyclic thiones using DMSO as the oxidant (**Scheme 5.6** (**c**)).[31]

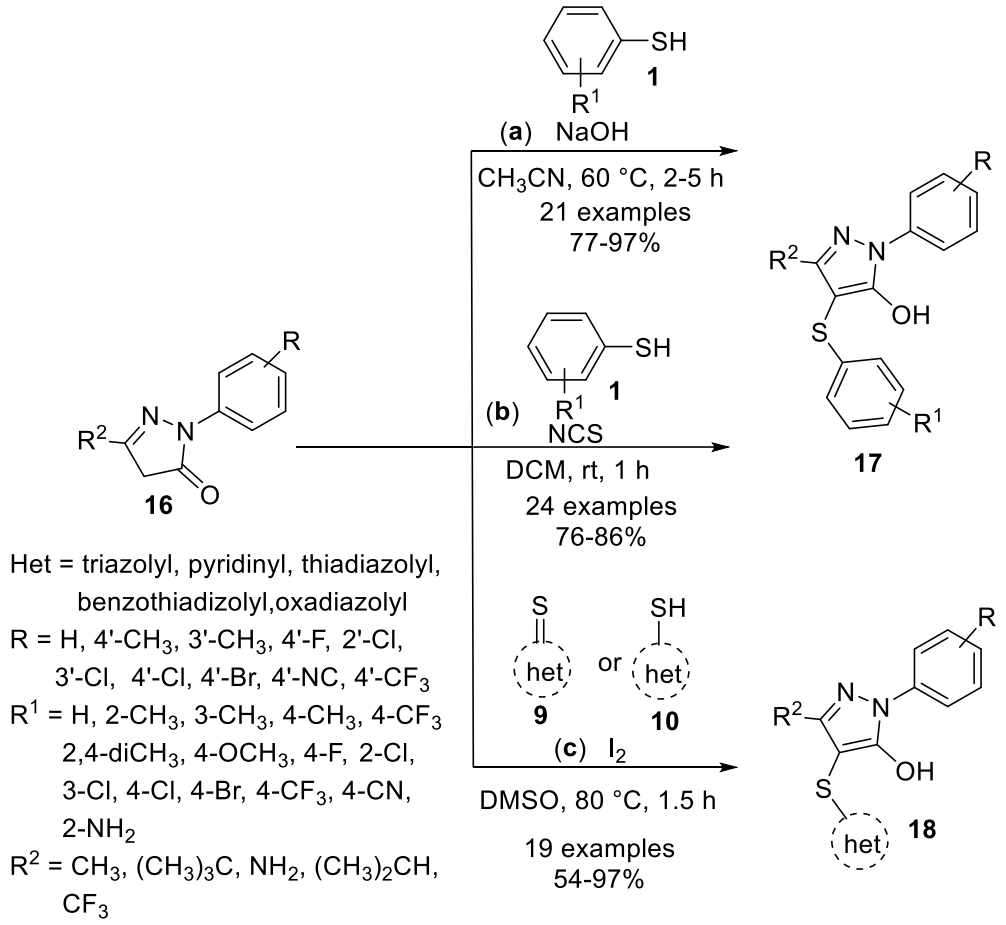

Scheme 5.6 Cross-dehydrogenative sulfenylation of pyrazolone

5.1.3 Transition Metal-free Cross-Dehydrogenative Sulfenylation of *N*-Heterocycles

The synthesis of heterocyclic thioethers has emerged as an intriguing strategy for the development of biologically active molecules.[32-33] Guo and co-workers reported an efficient and convenient photocatalytic direct C-3 sulfenylation of indoles (**19**) with thiophenols (**1**) for the construction of 3-sulfenylated indoles (**20**) using rose bengal as a photocatalyst (**Scheme 5.7** (**a**)). The reaction was believed to progress through rose bengal-assisted single electron transfer mechanism to form thiyl radical which underwent oxidative radical substitution reaction with indole to afford final

compounds. The uses of an inexpensive and readily available organic dye rose bengal as the photocatalyst and air as the terminal oxidant makes the protocol practical and environmentally benign.[34] Liu *et al*. performed the sulfenylation of indoles using simple iodine salt KIO_3 as a catalyst in DMSO:H_2O system. The reaction followed ionic mechanism involving the formation of polyvalent indole iodonium intermediate from the interaction of **19** and KIO_3. The polyvalent indole iodonium intermediate next underwent elimination of KOH, the addition of thiols (**1**) followed by reductive elimination resulted in the final product **20** in good yields (**Scheme 5.7** (**b**)).[35]

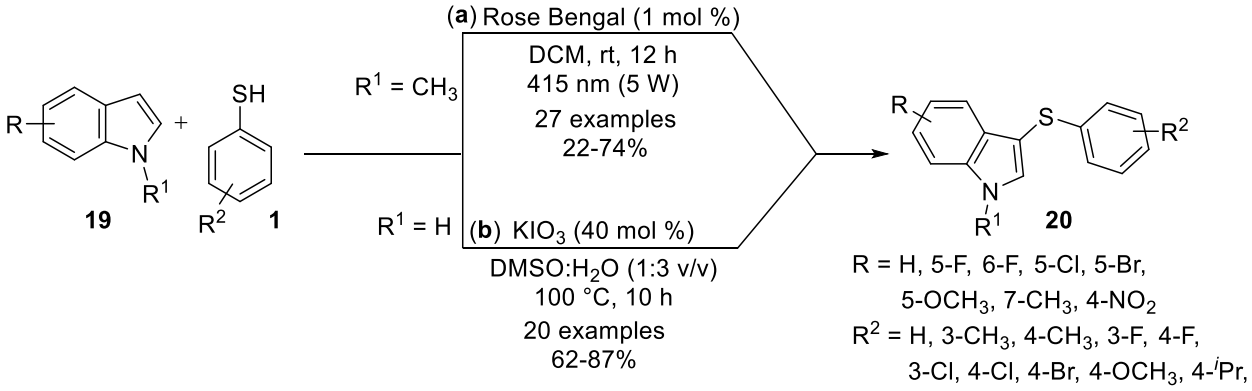

Scheme 5.7 Synthesis of C-3 sulfenylated indole derivatives

Cao and Zhao *et al.* developed efficient reagent controlled regioselective C(sp^2)−H cross-coupling of indolizines (**21**) with thiols (**1**) to synthesize mono/di sulfenylated indolizines by tuning the reagents. When the reaction of indolizines with **1** was performed in the presence of H_2O_2 monothiolation products (**23**) were obtained while the reaction in the presence of KI and TBHP resulted in dithiolated indolizines (**22**). The monothiolation reaction proceeded through single electron transfer (SET) mechanism by hydrogen peroxide-assisted formation of sulfide radical. The ionic mechanism was proposed for a dithiolation process involving disulfide intermediate which in presence of KI and DMSO underwent a double coupling reaction with indolizine to give 1,3-disulfenylated indolizines (**22**) (**Scheme 5.8**).[36]

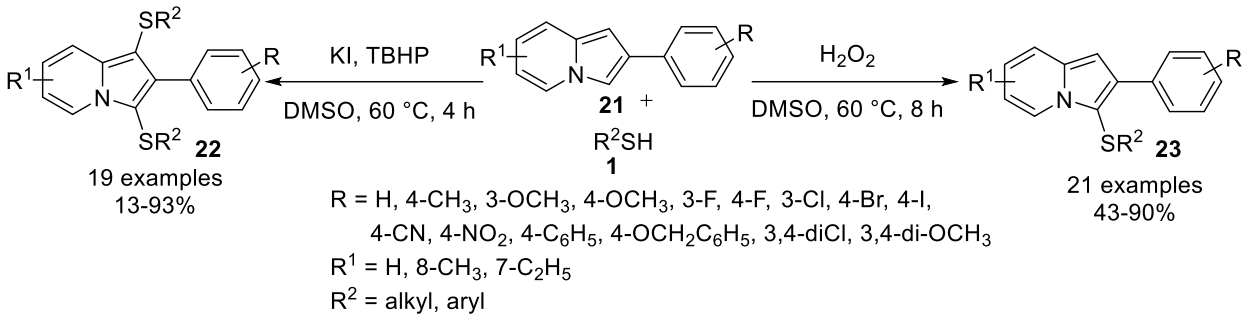

Scheme 5.8 Synthesis of mono/disulfenyalted indolizines

Wang *et al.* developed a green and efficient iodine-catalyzed cross-dehydrogenative C–S coupling method for the synthesis of C–4 sulfenylated pyrazoles (**25**) using DMSO as oxidant and solvent. A series of potential biologically active C–4 sulfenylated pyrazole frameworks were obtained in good to excellent yields. Presumably, the reaction followed ionic mechanism. The *in situ* formed sulfenyl iodide from thiol (**1**) underwent electrophilic substitution reaction on pyrazole (**24**) to afford the **25**. The broad substrate scope, metal-free approach and easy work up procedure were the noted advantages of the protocol (**Scheme 5.9**).[37]

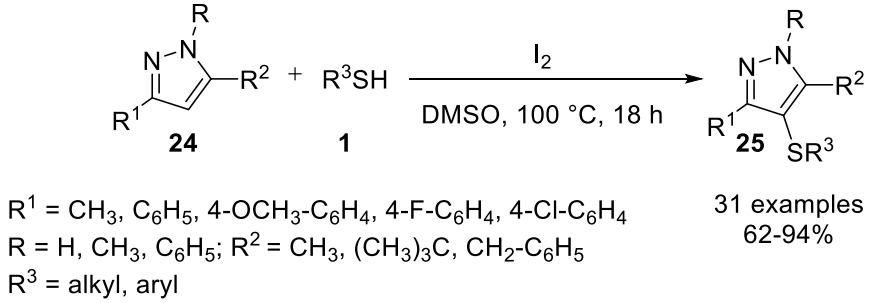

Scheme 5.9 Iodine-catalyzed synthesis of 4-sulfenylated pyrazoles

The compounds containing imidazo[1,2-*a*]pyridines framework have been of special interest since these structural motifs frequently occur in bioactive compounds and constitute the core structure of many commercially available drugs.[38-40] For example, the C-3 sulfonyl/sulfenyl imidazo[1,2-*a*]pyridine scaffolds (A and B) are found to inhibit Human Rhinovirus and helminths/parasitic activities respectively (Fig 1).[41]

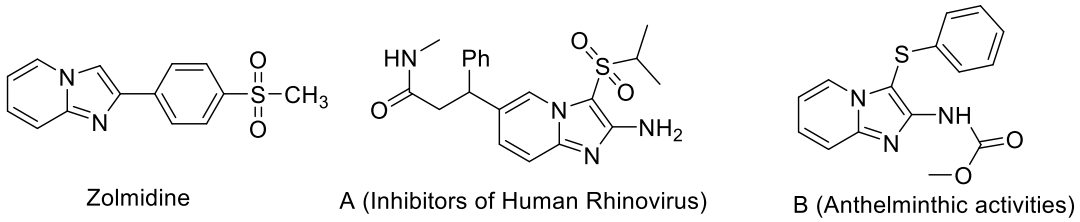

Figure 5.2 Biologically important scaffolds containing imidazo[1,2-*a*]pyridine and sulfur units

Over a couple of years, a surge in the literature documentation for the sulfenylation of imidazo[1,2-*a*]pyridines using different synthetic protocols have been observed.[42-44] The sulfenylation at the C-3 position of imidazo[1,2-*a*]pyridine is accomplished using various sulfenylating agents such as sulfonyl chlorides,[45] sulfonyl hydrazines or *S*-phenyl benzenesulfonothioate[46] and disulfides.[47] Moreover, sulfenylation of imidazo[1,2-*a*]pyridine is also explored by employing reagents such as silica-supported $CeCl_3.7H_2O$/NaI,[48] DMSO–$POCl_3$,[49] I_2/iodine reagents,[50-51] copper catalyst,[52-53] and *N*-chlorosuccinamide[54]. Despite the fact that there is a wide range of methods available for sulfenylation of imidazo[1,2-*a*]pyridine, these methods are limited because most of the existing methods rely on the use of functionalized sulfenylating agents, transition-metal, excess reagents, and harsh reaction conditions.

In this regard, transition-metal-free direct cross-dehydrogenative coupling reaction of thiols (**1**) with imidazo[1,2-*a*]pyridine (**26**) to construct sulfenylated imidazo[1,2-*a*]pyridine is an alternate environmentally benign method. Adimurthy *et al.* attempted the *N*-chlorosuccinimide-promoted cross-dehydrogenative sulfenylation of imidazo[1,2-*a*]pyridine (**26**) with **1** at room temperature to synthesize 2-phenyl-3-(phenylthio)imidazo-[1,2-*a*]pyridine (**27**) (**Scheme 5.10**). Initially, the reaction of NCS with benzenethiol (**1**) formed sulfenyl chloride *in situ*, subsequently, regioselective electrophilic attack at C-3 position of imidazo[1,2-*a*]pyridine (**26**) formed an imidazolenium intermediate. Finally, dehydrochlorination of intermediate provided the **27**. The scope of the methodology was extended to sulfenylation of imidazo[2,1-*b*]thiazoles and 2-phenylbenzo[*d*]imidazo[2,1-*b*]thiazole derivatives.[54]

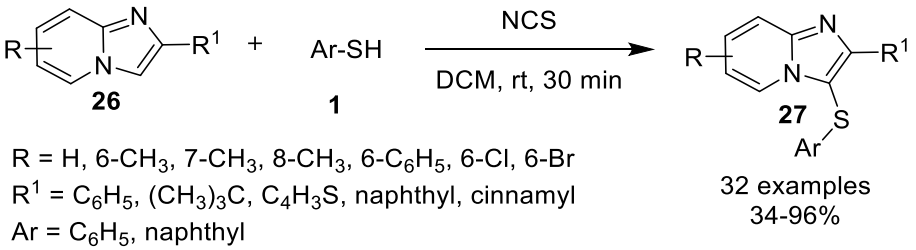

Scheme 5.10 NCS-promoted cross-dehydrogenative sulfenylation of imidazo[1,2-*a*]pyridine

Prabhu and co-workers disclosed cross-dehydrogenative coupling strategy for the C-3 sulfenylation of 2-arylimidazo[1,2-*a*]pyridines (**26**) from a variety of easily available heterocyclic thiols or thiones (**9** or **10**), using iodine as catalyst and dimethyl sulfoxide as an oxidant good to excellent yields (**Scheme 5.11** (**a**)).[55] Similarly, Hiebel *et al.* also reported iodine-catalyzed regioselective sulfenylation of imidazo[1,2-*a*]pyridines with various thiophenols (**1**) in PEG-400, using hydrogen peroxide as an oxidizing agent (**Scheme 5.11** (**b**)).[51] Very recently, Iida *et al.* documented use of a flavin-and-iodine dual catalytic system for sulfenylation of imidazo[1,2-*a*]pyridines with thiols under aerobic condition (**Scheme 5.11** (**c**)).[56]

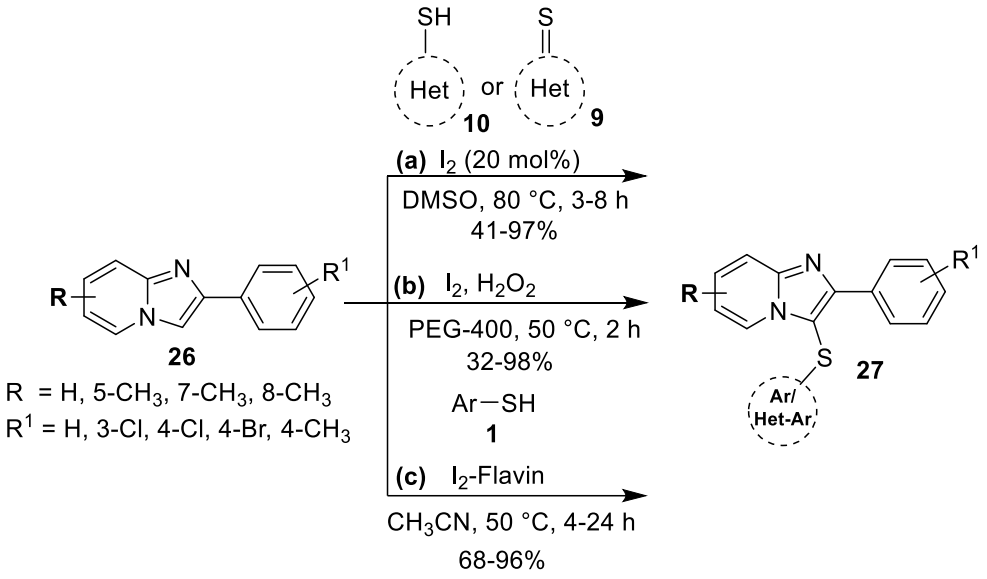

Scheme 5.11 I_2-mediated C-3 thioarylation/heterothioarylation of imidazo[1,2-*a*]pyridine

Barman and co-workers synthesized sulfenylated imidazo[1,2-*a*]pyridines (**27**) *via* visible-light-induced cross-dehydrogenative C(sp^2)–S coupling reaction between imidazo[1,2-*a*]pyridine (**26**) and thiols in presence of Rose Bengal as photocatalyst and blue LED as light source. The reaction

was believed to progress through Rose Bengal-assisted single electron transfer (SET) mechanism to form radical cation of thiol which eventually lost a proton to form thiyl radical and underwent radical substitution reaction with imidazo[1,2-*a*]pyridine (**26**) to afford final compounds. The thiols containing electron donating or withdrawing groups as well as aliphatic thiols reacted well under optimized reaction conditions.[57]

Scheme 5.12 Visible-light-induced C-3 sulfenylation of imidazo[1,2-*a*]pyridines

Additionally, the hydroxyl functional group is ubiquitous in natural products and medicinally important molecules.[58-59] It is also an important building block for constructing natural products, pharmaceutical, and medicinal compounds, as well as in polymers and materials.[60] Hence, the inclusion of C-S bond and -OH functional group in organic molecules in single maneuver would benefit in exploring interesting applications of new molecules.

Against this background, an approach which involves simultaneous formation of the sulfenylated imidazo[1,2-*a*]pyridine along with introduction of hydroxyl group in one maneuver offers an advantage in a way to design a mild, efficient and diversified method. As part of our growing interest towards the synthesis of imidazo[1,2-*a*]pyridine from 2-aminopyridinium salts,[61-62] in this chapter, we explored the base-mediated intramolecular amidation of 2-amino functionalized pyridinium salts followed by C(sp^3)−H cross-dehydrogenative coupling reaction with thiols leading to the formation of 2-hydroxy-3-sulfenylimidazo[1,2-*a*]pyridines.

5.2 RESULTS AND DISCUSSION

5.2.1 Optimization of Reaction Conditions

The preliminary studies began with the reaction of *p*-methylbenzenethiol (**1b**, 1.0 equiv.) and 2-amino-1-(2-ethoxy-2-oxoethyl)pyridinium bromide (**28a**, 1.2 equiv.) with NaOH (1.5 equiv.) in acetonitrile as solvent at 60 °C with stirring for 12 h. The reaction led to the formation of 2-

hydroxy-3-sulfenylimidazo[1,2-*a*]pyridine (**29ab**) in 51% yields (**Table 4.1**, entry 1). Initially, the role of the base on the outcome of the reaction was observed by employing different organic (**Table 4.1**, entries 7-10) and inorganic bases (**Table 4.1**, entries 1-6). Among all the bases screened, KOH was found to be working effectively giving desired product **29ab** in 61% yield (**Table 4.1**, entry 2). Considering the better yields obtained in KOH base, further optimization/control experiments proceeded with the same base. Next, the compatibility of other solvents for current transformation was examined. The reaction in THF and 1,4-dioxane gave the product **29ab** in 52% and 48% yields respectively, whereas the toluene was found to be detrimental to product formation (**Table 4.1**, entries 11-13). The reaction in water was also satisfactory and produced the product **29ab** in 50% yield (**Table 4.1**, entry 14). The absence of KOH inhibited the reaction performance (**Table 4.1,** entry 15). Variable-temperature experiments employing ACN as solvent and KOH as base revealed that the yield of **29ab** reduced to 52% and 35% yield at 80 °C and 100 °C, respectively, whereas lowering the temperature resulted in increase in the yield of **29ab** to 73% at 30 °C (**Table 4.1,** entries 16-18). Thus the best reaction condition for model reaction obtained was use of 1.2 equiv. of salt (**28a**) reacted with 1 equiv. of thiol (**1b**) in presence of KOH (1.5 equiv.) in acetonitrile (5 mL) at room temperature under air atmosphere, for 12 h (**Table 4.1,** entry 16).

Table 5.1 Optimization of the reaction conditions for the synthesis of **29ab**[a]

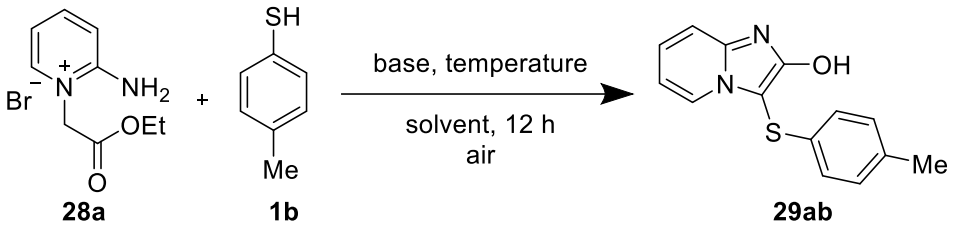

28a **1b** **29ab**

S. No.	Base (1.5 equiv.)	Solvent	Temperature (°C)	Yield of 29ab (%)[b]
1.	NaOH	CH_3CN	60	51
2.	KOH	CH_3CN	60	61
3.	K_2CO_3	CH_3CN	60	25

4.	K_3PO_4	CH_3CN	60	51
5.	Cs_2CO_3	CH_3CN	60	<5
6.	NaOAc	CH_3CN	60	10
7.	DBU	CH_3CN	60	n.d
8.	NEt_3	CH_3CN	60	51
9.	Piperidine	CH_3CN	60	Trace
10.	DMAP	CH_3CN	60	Trace
11.	KOH	THF	60	52
12.	KOH	1,4-dioxane	60	48
13.	KOH	Toluene	60	n.d
14.	KOH	H_2O	60	50
15.	-	CH_3CN	60	n.d
16.	**KOH**	**CH_3CN**	**30**	**73**
17.	KOH	CH_3CN	80	52
18.	KOH	CH_3CN	100	35

[a]The reaction was performed with 2-amino-1-(2-ethoxy-2-oxoethyl)pyridinium bromide (**28a**) (1.2 equiv.), *p*-methylbenzenethiol (**1b**) (1.0 equiv.), base (1.5 equiv.), solvent (5 mL), T °C temperature, air atmosphere, 12 h; [b]Isolated yields

5.2.2 Comparative Study

Meanwhile, we turned our attention towards the comparative study of other sulfenylating agents over thiophenol under optimized reaction condition (**Scheme 5.13**). Among studied agents, the reaction of 4-methylbenzenesulfonohydrazide provided 10% yield of **29ab** while sodium benzenesulfinate delivered 7% yield of **29aa** under optimized reaction condition. However, 4 methylbenzenesulfonyl chloride was found to be ineffective in reaction with 2-aminopyridinium salt (**28a**). 1,2-di-*p*-tolyldisulfane performed well as sulfenylating agent and successfully reacted

with **28a** to provide the desired product **29ab** in 70% yield which is comparable in respect to yield of **29ab** obtained using thiophenol (73%) as a sulfenylating agent.

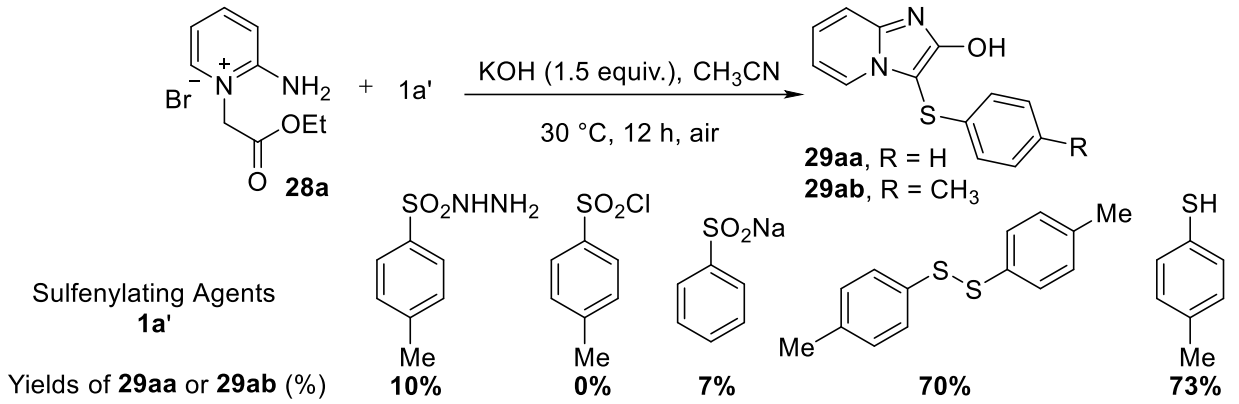

Scheme 5.13 Comparative study of different sulfenylating agents

5.2.3 Synthesis of 2-Hydroxy-3-sulfenylimidazo[1,2-*a*]pyridine

Under the optimized reaction conditions, various 2-aminopyridinium salts and thiphenols were used to investigate the generality of the tandem reaction, and a series of 2-hydroxy-3-sulfenylimidazo[1,2-*a*]pyridine were synthesized in moderate to excellent yields. As shown in table **5.2,** we first investigated the scope of thiophenols (**1a-i**) with 2-aminopyridinium salts (**28a**). The thiophenol (**1a**) led to 63% yield of desired product (**29aa**) while reaction with 4-methylthiophenol (**1b**) resulted 73% yield (**29ab**). Gratifyingly, halogen substituted (4-chloro, 4-bromo and 2-bromo) thiophenols (**1c, 1d** and **1h**) reacted smoothly under the optimized reaction condition to give corresponding sulfenylated imidazo[1,2-*a*]pyridine-2-ols (**29ac**, **29ad** and **29ah**) in goodyields. The halo-substituent on the aryl ring could be utilized in further functionalization. Moreover, reaction with 3-methoxythiophenol (**1e**) and 4-methoxythiophenol (**1f**) underwent smoothly leading to 70% and 56% yields of respective desired products (**29ae** and **29af**). Additionally, 78% yield of respective product was obtained by the reaction of 4-nitrothiophenol (**1g**) and 2-aminopyridinium salt (**28a**). On the other hand, aliphatic and heterocyclic thiols were not tolerated under optimized reaction condition. The position of substituents on pyridinium salts influenced the reaction outcome, for example, slightly lower yields of the desired product were obtained from the C-5 methyl/aryl substituted 2-aminopyridinium salts (**28d, 28g** and **28h**) whilst C-5 halogen substituted 2-aminopyridinium salts (**28e** and **28f**) led to improved yields of desired products.

Table 5.2 Substrate scope for synthesis of 2-hydroxy-3-sulfenylimidazo[1,2-*a*]pyridines.[a,b]

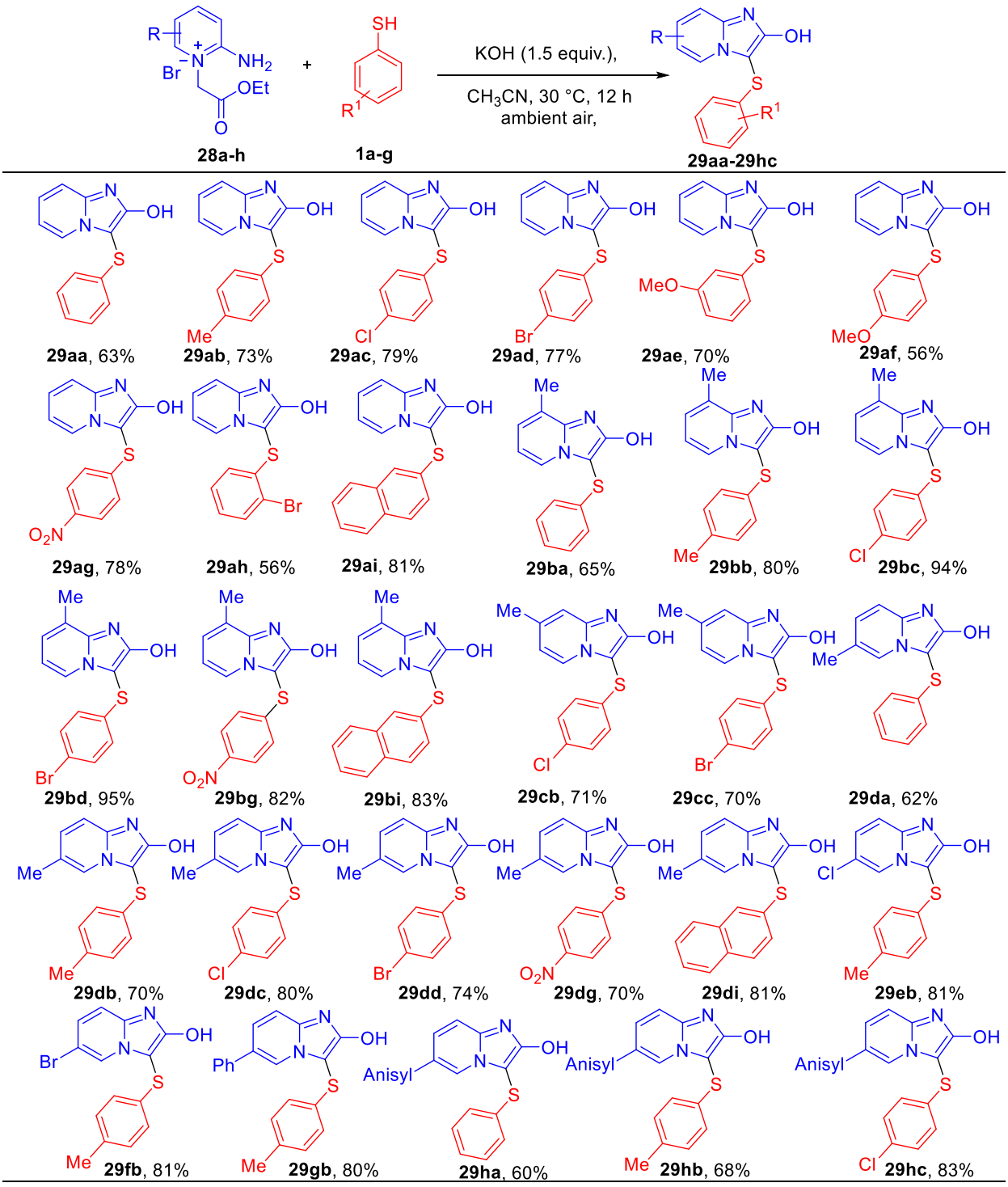

[a]The reaction was performed with 2-amino-1-(2-ethoxy-2-oxoethyl)pyridinium bromide (1.2 equiv.), thiol (1.0 equiv.), KOH (1.5 equiv.), CH_3CN (5 mL), 30 °C, air atmosphere, 12 h; [b]Isolated yields

Structures of all the synthesized compounds were elucidated by IR, ^{1}H NMR, ^{13}C NMR, and HRMS analysis. In the ^{1}H NMR spectrum of **29ab**, the characteristic broad singlet for –OH proton appeared at δ 11.79 ppm and $-CH_3$ protons were observed at δ 2.21 ppm along with other peaks in aromatic region (**Figure 5.3**). In the ^{13}C NMR spectrum of **29ab**, the presence C-O carbon at δ 161 ppm and methyl at carbon δ 20.9 ppm along with all other corresponding carbon peaks were observed (**Figure 5.4**).

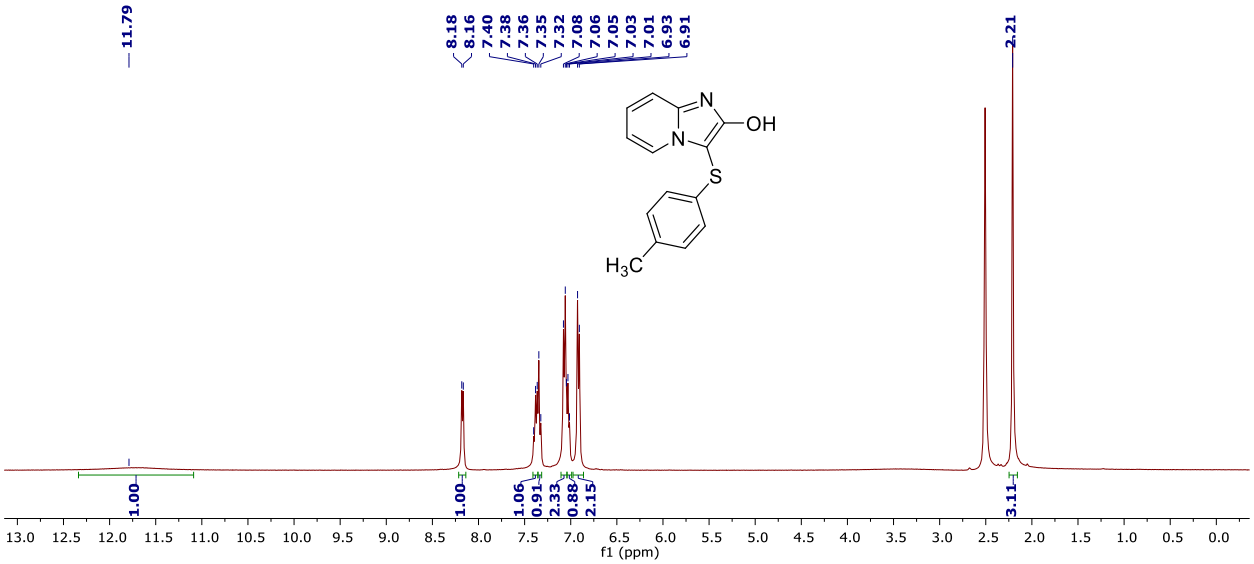

Figure 5.3 ^{1}H NMR spectrum of **29ab**

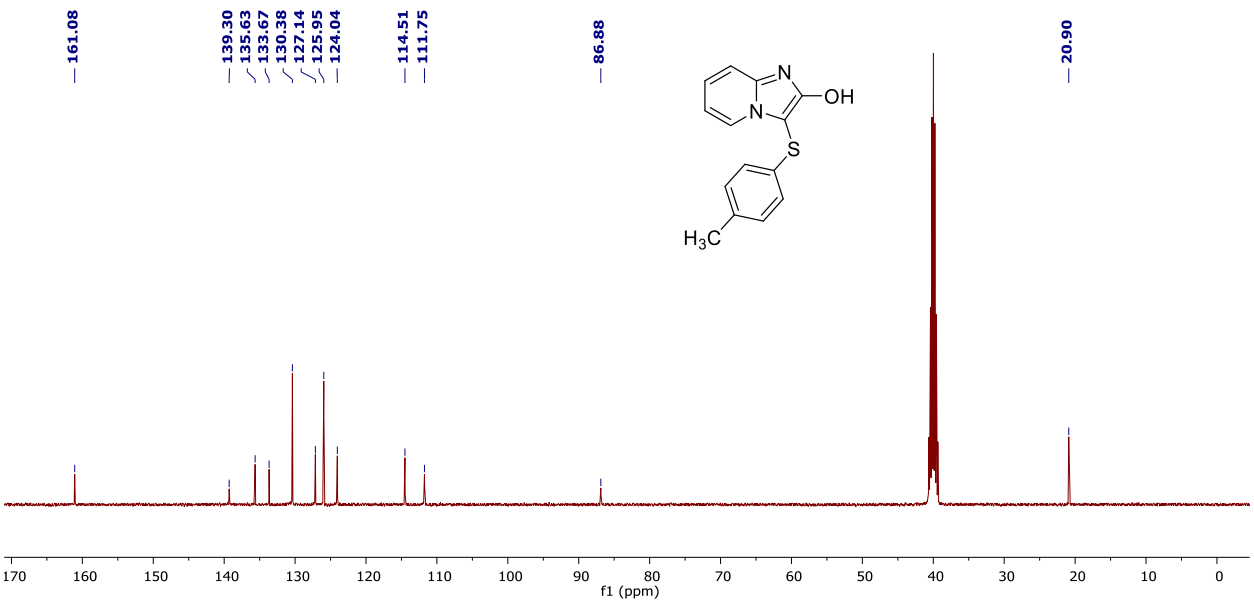

Figure 5.4 ^{13}C NMR spectrum of **29ab**

The structure of the product **29ad** (CCDC 1882988) was unambiguously determined by single X-ray diffraction analysis (**Figure 5.5**). The probability of hydrogen migration from oxygen to nitrogen was observed leading to a zwitter ionic molecule which was susceptible to form a dimer *via* intermolecular hydrogen bonding with another molecule during the crystallization process. This phenomenon was also observed during NMR recording of the products, for some of the molecules the peak corresponding to hydroxyl group was not observed.

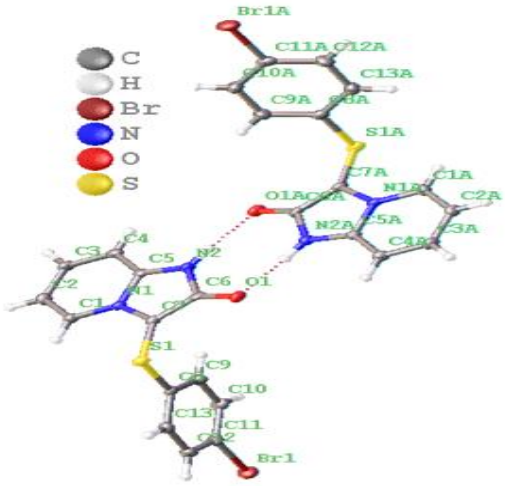

Figure 5.5 ORTEP diagram of **29ad**. The displacement ellipsoids are drawn at 50% probability level.

5.2.4 Synthetic Application

The presence of hydroxyl functionality in the molecule was utilized for further functionalization of the molecule. The **29ab** was subjected to tosylation reaction followed by Suzuki coupling reaction with arylboronic acids to synthesize three examples of 2-aryl-3-sulfenylimidazo[1,2-*a*]pyridine derivatives (**31**). Initially, the C-2 hydroxylated product **29ab** was treated with *p*-toluenesulfonyl chloride in triethylamine in DCM at room temperature to obtain the C-2 tosylated product. Subsequently, the tosylated product was treated with different arylboronic acids (**30**) in the presence of $Pd(OAc)_2$, K_3PO_4 in ethylene glycol to obtain the Suzuki cross coupled products **31a-31c** in good yields.

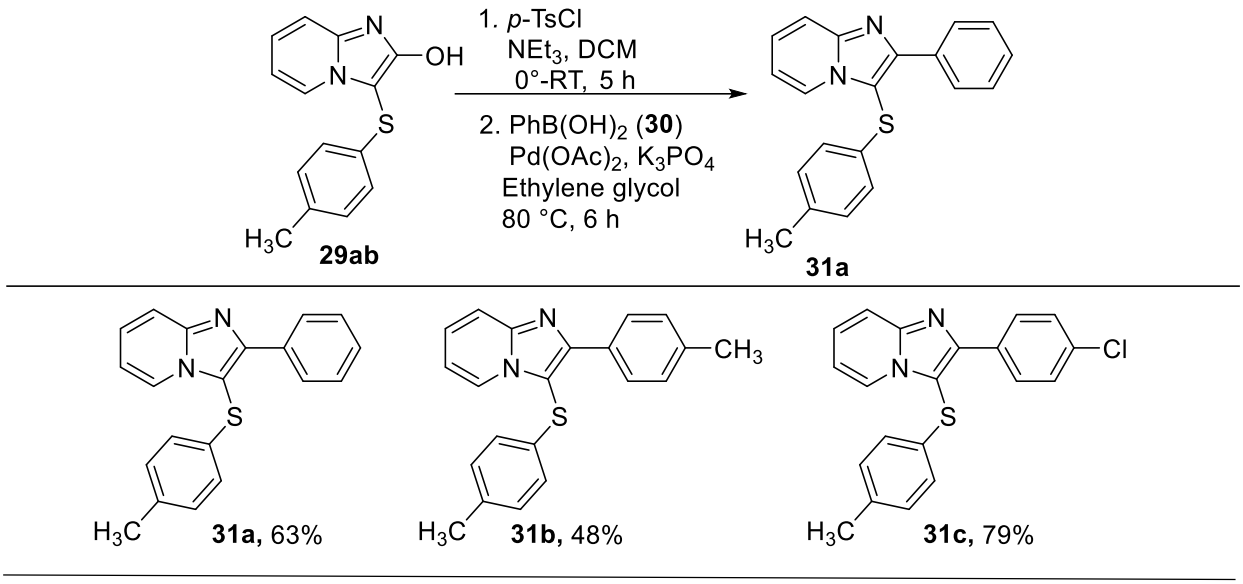

Scheme 5.14 Synthetic application

5.2.4 Control Experiments

To explore the mechanism involved in this transformation, we executed a set of control experiments. At first, desired product formation was not observed when the reaction of **1b** and **28a** was performed in the absence of a base (**Scheme 5.15** (**a**)). When **1b** was subjected to optimized reaction conditions in the absence of **28a**, formation of 1,2-di-*p*-tolyldisulfane **(32)** was obtained within 30 min of commencement of reaction (**Scheme 5.15** (**b**)). Similarly, the base-catalyzed reaction of **28a** led to the formation of **33** in 50% yield (**Scheme 5.15** (**c**)). Subsequently, the reaction of **1b** and **33** under optimized reaction conditions produced the desired product **29ab** in 75% yield (**Scheme 5.15** (**d**)). Likewise, the reaction of 1,2-di-*p*-tolyldisulfane **(32**) and **28a** under the standard conditions gave **29ab** in 70% yield (**Scheme 5.15** (**e**)). Both the reaction indicated the possibility of **32** and **33** as reaction intermediates. However, the reaction of **1b** and **28a** under inert reaction condition failed to yield desired product, while the reaction of **32** with **1a** under similar condition provided 68% yield of desired product (**Scheme 5.15** (**f**)-(**g**)). These outcomes showed that **32** might be another probable reaction intermediate in the reaction. The presence of air is required for the formation of **32**.

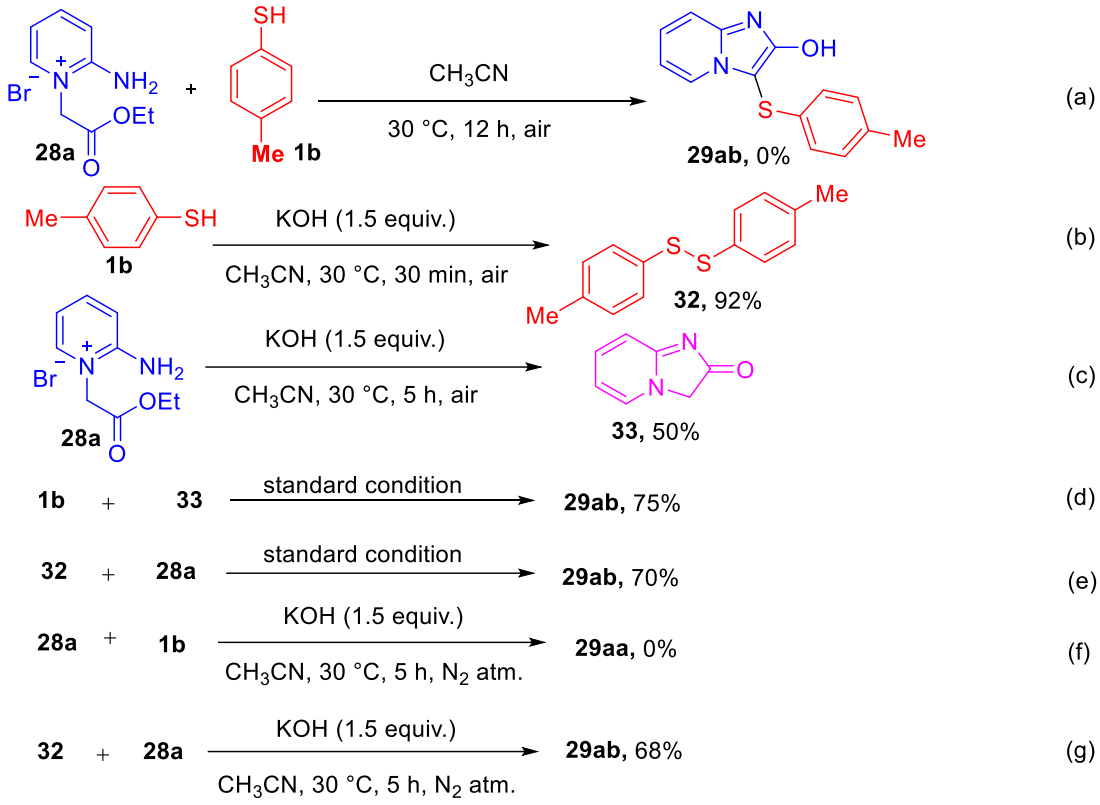

Scheme 5.15 Control experiments

Additionally, a set of radical scavenging experiments were performed to understand the mechanism pathway (**Scheme 5.16**). When the reaction was performed in the presence of radical scavengers such as TEMPO and DPE the product formation was quenched substantially while in case of BHT, the **29ab** was isolated in 25% yields. The observation indicated the possibility of the radical mechanism. Moreover, the crude reaction mass performed with TEMPO was analyzed in ESI-HRMS using $CH_3CN:H_2O$ (6:4) solvent system to observe a TEMPO adduct corresponding to the sulfide radical at *m/z* 280.1721 (calcd *m/z* 280.1730) (**Figure 5.6**).

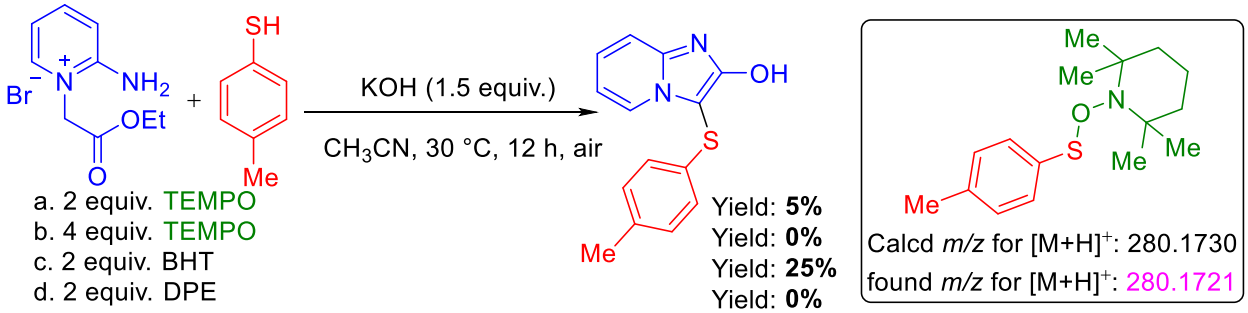

Scheme 5.16 Radical Scavenging experiments

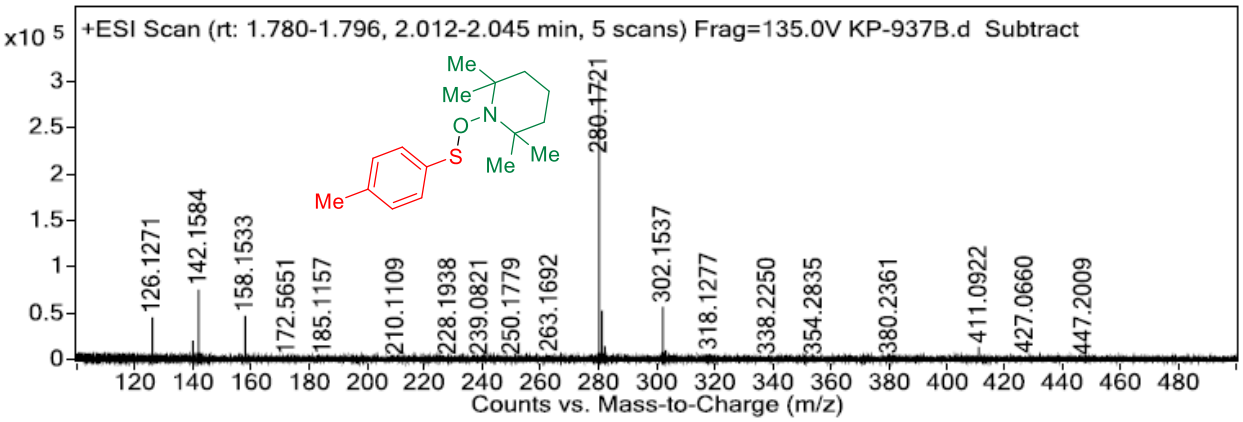

Figure 5.6 The ESI-HRMS profile for the crude reaction mass performed with TEMPO

5.2.5 Plausible Mechanism

Based on investigative reaction outcomes and the literature reports,[63] a probable reaction mechanism for the formation of **29** is shown in scheme **5.17**. Initially, 2-aminopyridinium salt (**28)** in the presence of base undergoes intramolecular amidation reaction to from **33**, which subsequently on deprotonation of CH_2 protons converts into an electron rich enolate anion potassium salt **A.** On the other hand, thiols (**1**) on aerial oxidation converts into reactive thiyl radical cation **B** which in the presence of base formed disulfide (**32**). The radical **B** formation was supported by the observation of TEMPO adduct at *m/z* 280.1721 (calcd *m/z* 280.1735) in HRMS analysis of reaction mixture. Finally, the nucleophilic attack of the *in situ* generated enolate **A** on disulfide **32** affords 3-sulfenylated imidazo[1,2-***a***]pyridine-2-one (**C**) which on tautomerization converts to more stable 3-sulfenylated imidazo[1,2-*a*]pyridine-2-ol (**29**).

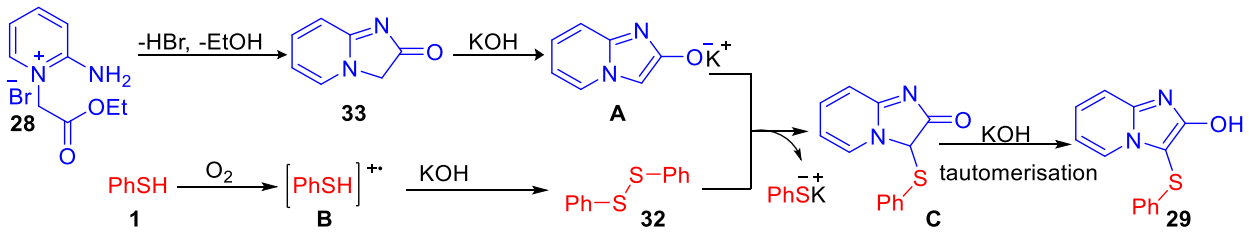

Scheme 5.17 Proposed mechanism for formation of 3-sulfenylated imidazo[1,2-*a*]pyridine-2-ol

5.3 CONCLUSIONS

In conclusion, a new and efficient method for the synthesis of 2-hydroxy-3-sulfenylimidazo[1,2-*a*]pyridine from readily available starting materials under ambient reaction condition. The *in situ*

enolate anion of amidation product allows facile base-mediated cross-dehydrogenative coupling reaction of active methylene group and thiols. This new method allows the synthesis of diverse 2-hydroxy-3-sulfenylimidazo[1,2-*a*]pyridines in good to excellent yields. Further studies of biological activities of new molecules and design of new molecules *via* further reactions of these structural motifs are in progress in our laboratory.

5.4 EXPERIMENTAL SECTION

5.4.1 Materials and Methods

All reagents and solvents were purchased from commercial sources and used without further purification. Melting points were measured using an automatic capillary point apparatus and are uncorrected. The thin layer chromatography (TLC) was performed on 0.25 mm silica gel 60-F254, and a UV lamp was used as a visualizing agent. Column chromatography was performed using silica gel (100−200 mesh), and hexane and ethyl acetate were used as eluents. The ^{1}H and ^{13}C NMR spectra were obtained on a 400 and 100 MHz spectrometer. Coupling constants and chemical shifts were reported in hertz (Hz) and parts per million (ppm), respectively, relative to the internal standard of tetramethylsilane (TMS). IR spectroscopy was performed as a neat sample on an FT-IR instrument, and values are expressed in cm^{-1}. The HRMS were analyzed by the electrospray ionization (ESI) method in positive mode on a Q-TOF LC-MS spectrometer. The synthesis of 2-aminopyridinium bromides was achieved from the reaction of corresponding 2-aminopyridine and ethyl bromoacetate following our earlier reported method.[62]

5.4.2 Representative Procedure for the Synthesis of 2-Hydroxy-3-sulfenylimidazo[1,2-*a*]pyridines (29aa-29hc)

An oven-dried 10 mL round bottom flask was charged with 2-amino-1-(2-ethoxy-2-oxoethyl)pyridin-1-ium bromide (0.156 g, 0.600 mmol), 4-methylthiophenol (0.062 g, 0.500 mmol), and KOH (0.042 g, 0.750 mmol) in acetonitrile (5 mL). The resulting reaction mixture was stirred at 30 °C for 12 h. The reaction was monitored by TLC over the time. On completion of the reaction, acetonitrile was evaporated under reduced pressure to obtain a residue. Water was added to the residue and neutralized with 2N HCl to obtain a solid precipitate. The precipitate was vacuum filtered and dried to obtain crude brown solid. The crude residue was subjected to column

chromatography (EtOAc: hexane, 1:1 *v/v*) to afford **29ab** in 73% (0.093 g) yield as a cream colored solid.

3-(Phenylthio)imidazo[1,2-a]pyridin-2-ol (29aa).

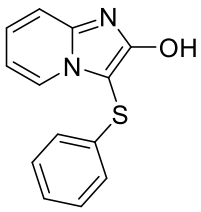

Brown colored solid (0.093 g, 77%); MP 289 – 291 °C; ^{1}H NMR (400 MHz, DMSO-d_6) δ 11.77 (bs, 1H), 8.20 (d, J = 6.5 Hz, 1H), 7.40 (ddd, J = 8.4, 6.9, 1.3 Hz, 1H), 7.37 – 7.31 (m, 1H), 7.26 (t, J = 7.7 Hz, 2H), 7.18 – 7.11 (m, 1H), 7.04 (td, J = 6.8, 1.5 Hz, 1H), 7.02 – 6.96 (m, 2H); ^{13}C NMR (100 MHz, DMSO-d_6) δ 161.1, 139.3, 137.3, 129.7, 127.3, 126.1, 125.4, 124.1, 114.6, 111.6, 86.1; FT-IR ν_{max} (neat) 3564, 3074, 2916, 1612, 1465, 1327, 1265, 1149, 1018, 887, 732 cm^{-1}; HRMS (ESI-TOF, *m/z*): calcd for $C_{13}H_{11}N_2OS$ $[M + H]^+$ 243.0587, found 243.0590.

3-(p-Tolylthio)imidazo[1,2-a]pyridin-2-ol (29ab).

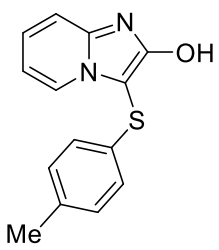

Cream colored solid (0.093 g, 73%); MP 208 – 210 °C; ^{1}H NMR (400 MHz, DMSO-d_6) δ 11.76 (bs, 1H), 8.17 (d, J = 6.6 Hz, 1H), 7.38 (t, J = 7.7 Hz, 1H), 7.34 (d, J = 8.5 Hz, 1H), 7.07 (d, J = 7.9 Hz, 2H), 7.02 (d, J = 6.7 Hz, 1H), 6.92 (d, J = 7.8 Hz, 2H), 2.21 (s, 3H); ^{13}C NMR (100 MHz, DMSO-d_6) δ 161.0, 139.3, 135.6, 133.6, 130.3, 127.1, 125.9, 124.0, 114.5, 111.7, 86.8, 20.9; FT-IR ν_{max} (neat) 3364, 3086, 2916, 1612, 1585, 1435, 1265, 1157, 1018, 740 cm^{-1}; HRMS (ESI-TOF, *m/z*): calcd for $C_{14}H_{13}N_2OS$ $[M + H]^+$ 257.0743, found 257.0725.

3-((4-Chlorophenyl)thio)imidazo[1,2-a]pyridin-2-ol (29ac).

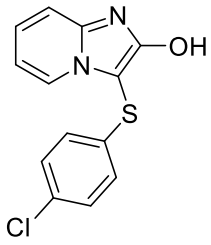

Off-white solid (0.109 g, 79%); MP 220 – 222 °C; ^{1}H NMR (400 MHz, DMSO-d_6) δ 11.90 (bs, 1H), 8.23 – 8.15 (m, 1H), 7.42 (ddd, J = 8.4, 7.0, 1.3 Hz, 1H), 7.37 – 7.30 (m, 3H), 7.07 (dd, J = 6.8, 1.3 Hz, 1H), 7.02 (d, J = 8.6 Hz, 2H); ^{13}C NMR (100 MHz, DMSO-d_6) δ 161.0, 139.2, 136.6, 130.7, 129.6, 127.6, 127.2, 124.1, 114.8, 111.4, 85.4; FT-IR ν_{max} (neat) 3356, 3062, 1643, 1612, 1512, 1465, 1327, 1265, 1111, 756 cm^{-1}; HRMS (ESI-TOF, *m/z*): calcd for $C_{13}H_{10}ClN_2OS$ $[M + H]^+$ 277.0197, found 277.0203.

3-((4-Bromophenyl)thio)imidazo[1,2-a]pyridin-2-ol (29ad).

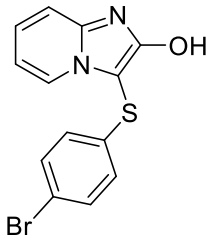

Off-white solid (0.123 g, 77%); MP 245 – 247 °C; ^{1}H NMR (400 MHz, DMSO-d_6) δ 11.87 (bs, 1H), 8.19 (d, J = 6.6 Hz, 1H), 7.45 (d, J = 8.2 Hz, 2H), 7.41 (d, J = 7.6 Hz, 1H), 7.34 (d, J = 8.6 Hz, 1H), 7.06 (t, J = 6.8 Hz, 1H), 6.95 (d, J = 8.2 Hz, 2H); ^{13}C NMR (100 MHz, DMSO-d_6) δ 161.0, 139.1, 137.2, 132.5, 127.6, 127.5, 124.1, 118.9, 114.8, 111.4, 85.3; FT-IR ν_{max} (neat) 3564, 3062, 1612, 1419, 1327, 1265, 1211, 1111, 756 cm^{-1}; HRMS (ESI-TOF, *m/z*): calcd for $C_{13}H_{10}BrN_2OS$ $[M + H]^+$ 320.9692, 322.9671, found 320.9667, 322.964.

3-((3-Methoxyphenyl)thio)imidazo[1,2-a]pyridin-2-ol (29ae).

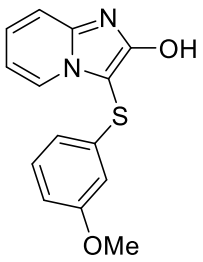

Off-white solid (0.095 g, 70%); MP 262 – 264 °C; ^{1}H NMR (400 MHz, DMSO-d_6) δ 11.73 (s, 1H), 8.19 (d, J = 6.6 Hz, 1H), 7.40 (t, J = 7.8 Hz, 1H), 7.35 (d, J = 8.5 Hz, 1H), 7.17 (t, J = 8.0 Hz, 1H), 7.05 (t, J = 6.5 Hz, 1H), 6.72 (dd, J = 8.3, 2.5 Hz, 1H), 6.55 (s, 1H), 6.53 (d, J = 8.0 Hz, 1H), 3.67 (s, 3H); ^{13}C NMR (100 MHz, DMSO) δ 161.1, 160.3, 139.2, 138.8, 130.7, 127.4, 124.1, 117.5, 114.6, 111.5, 111.1, 86.1, 55.5; FT-IR ν_{max} (neat) 3363, 2916, 1609, 1582, 1481, 1327, 1265, 1111, 1084, 756 cm^{-1}; HRMS (ESI-TOF, *m/z*): calcd for $C_{14}H_{13}N_2O_2S$ $[M + H]^+$ 273.0692, found 273.0670.

3-((4-Methoxyphenyl)thio)imidazo[1,2-a]pyridin-2-ol (29af).

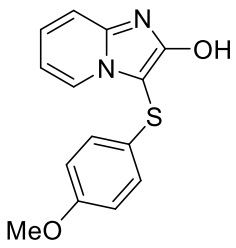

Off-white solid (0.076 g, 56%); MP 272 – 274 °C; ^{1}H NMR (400 MHz, DMSO-d_6) δ 11.77 (bs, 1H), 8.24 (d, J = 6.5 Hz, 1H), 7.37 (t, J = 8.1 Hz, 1H), 7.31 (d, J = 8.6 Hz, 1H), 7.04 (d, J = 8.1 Hz, 3H), 6.85 (d, J = 8.3 Hz, 2H), 3.68 (s, 3H); ^{13}C NMR (100 MHz, DMSO-d_6) δ 160.9, 158.5, 139.2, 128.4, 127.5, 127.0, 124.0, 115.4, 114.4, 111.8, 88.1, 55.6; FT-IR ν_{max} (neat) 3564, 3363, 2916, 1612, 1556, 1481, 1327, 1265, 1111, 1072, 1026, 758 cm^{-1}; HRMS (ESI-TOF, *m/z*): calcd for $C_{14}H_{13}N_2O_2S$ $[M + H]^+$ 273.0692, found 273.0677.

3-((4-Nitrophenyl)thio)imidazo[1,2-a]pyridin-2-ol (29ag).

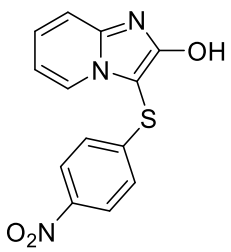

Yellow solid (0.112 g, 78%); MP 214 – 216 °C; ^{1}H NMR (400 MHz, DMSO-d_6) δ 11.95 (bs, 1H), 8.19 (dt, J = 6.6, 1.1 Hz, 1H), 8.14 – 8.07 (m, 2H), 7.47 (ddd, J = 8.5, 7.1, 1.2 Hz, 1H), 7.37 (dt, J = 8.7, 1.2 Hz, 1H), 7.25 – 7.18 (m, 2H), 7.08 (td, J = 6.9, 1.3 Hz, 1H); ^{13}C NMR (100 MHz, DMSO-d_6) δ 160.9, 147.8, 145.7, 128.2, 125.5, 124.8, 124.3, 115.1, 111.1, 99.9, 83.3; FT-IR ν_{max} (neat) 3394, 2989, 1612, 1481, 1373, 1265, 1118, 1076, 740 cm^{-1}; HRMS (ESI-TOF, *m/z*): calcd for $C_{13}H_{10}N_3O_3S$ $[M + H]^+$ 288.0437, found 288.0409.

3-((2-Bromophenyl)thio)imidazo[1,2-a]pyridin-2-ol (29ah).

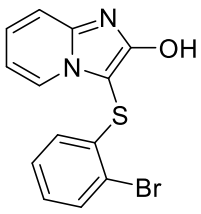

Off-white solid (0.090 g, 56%); ^{1}H NMR (400 MHz, DMSO-d_6) δ 11.90 (bs, 1H), 8.14 (d, J = 6.5 Hz, 1H), 7.63 (dd, J = 7.9, 1.3 Hz, 1H), 7.50 – 7.41 (m, 1H), 7.37 (d, J = 8.6 Hz, 1H), 7.20 (td, J = 7.6, 1.3 Hz, 1H), 7.14 – 7.06 (m, 1H), 7.06 (dd, J = 7.2, 1.3 Hz, 1H), 6.44 (dd, J = 7.8, 1.6 Hz, 1H); ^{13}C NMR (100 MHz, DMSO-d_6) δ 161.1, 139.2, 137.9, 133.5, 128.8, 127.9, 127.5, 125.5, 124.2, 119.4, 115.1, 111.2, 84.3; FT-IR ν_{max} (neat) 3564, 3086, 2916, 1612, 1565, 1435, 1327, 1265, 1157, 1018, 740 cm^{-1}; HRMS (ESI-TOF, *m/z*): calcd for $C_{13}H_{10}BrN_2OS$ $[M + H]^+$ 320.9692, 322.9671, found 320.9696, 322.9675.

3-(Naphthalen-2-ylthio)imidazo[1,2-a]pyridin-2-ol (29ai).

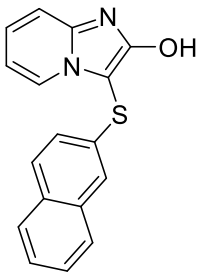

Off-white solid (0.118 g, 81%); MP 245 – 247 °C; ^{1}H NMR (400 MHz, DMSO-d_6) δ 11.84 (bs, 1H), 8.22 (d, J = 6.6 Hz, 1H), 7.84 (d, J = 9.3 Hz, 2H), 7.75 (d, J = 7.7 Hz, 1H), 7.50 (s, 1H), 7.45 (t, J = 7.1 Hz, 2H), 7.40 (d, J = 7.1 Hz, 1H), 7.36 (d, J = 8.7 Hz, 1H), 7.19 (d, J = 8.7 Hz, 1H), 7.03 (t, J = 6.8 Hz, 1H); ^{13}C NMR (100 MHz, DMSO-d_6) δ 161.1, 139.2, 134.9, 133.8, 131.7, 129.4, 128.1, 127.4, 127.3, 127.2, 126.0, 124.2, 124.1, 123.2, 114.7, 111.5, 86.0; FT-IR ν_{max} (neat) 3394, 2989, 1643, 1612, 1481, 1373, 1265, 1134, 1076, 740 cm^{-1}; HRMS (ESI-TOF, *m/z*): calcd for $C_{17}H_{13}N_2OS$ $[M + H]^+$ 293.0743 found 293.0750.

8-Methyl-3-(phenylthio)imidazo[1,2-a]pyridin-2-ol (29ba).

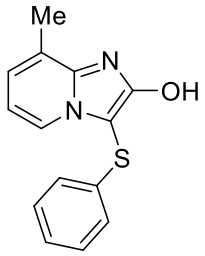

Off-white solid (0.083, 65%); MP 225 – 227 °C; ^{1}H NMR (400 MHz, DMSO-d_6) δ 11.82 (bs, 1H), 8.05 (d, J = 6.6 Hz, 1H), 7.25 (q, J = 7.2 Hz, 3H), 7.14 (t, J = 7.3 Hz, 1H), 6.98 (d, J = 8.2 Hz, 2H), 6.94 (d, J = 7.1 Hz, 1H), 2.42 (s, 3H); ^{13}C NMR (100 MHz, DMSO-d_6) δ 161.3, 139.5, 137.4, 129.7, 126.7, 126.1, 125.4, 121.9, 120.5, 114.2, 86.6, 16.2; FT-IR ν_{max} (neat) 3369, 3093, 1604, 1465, 1256, 1180, 756 cm^{-1}; HRMS (ESI-TOF, *m/z*): calcd for $C_{14}H_{13}N_2OS$ $[M + H]^+$ 257.0743, found 257.0745.

8-Methyl-3-(p-tolylthio)imidazo[1,2-a]pyridin-2-ol (29bb).

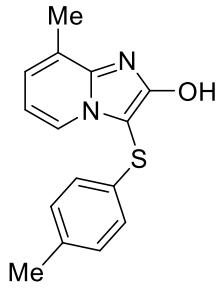

Off-white solid (0.076 g, 56%); MP 253 – 255 °C; ^{1}H NMR (400 MHz, DMSO-d_6) δ 11.71 (bs, 1H), 8.03 (d, J = 6.5 Hz, 1H), 7.22 (d, J = 7.2 Hz, 1H), 7.07 (d, J = 8.0 Hz, 2H), 6.94 (t, J = 6.9 Hz, 1H), 6.90 (d, J = 8.2 Hz, 2H), 2.41 (s, 3H), 2.21 (s, 3H); ^{13}C NMR (100 MHz, DMSO-d_6) δ 161.2, 137.3, 135.6, 133.7, 132.7, 130.3, 126.5, 125.9, 121.9, 114.1, 87.2, 20.9, 16.2; FT-IR ν_{max} (neat) 3564, 3074, 2962, 1643, 1604, 1572, 1442, 1327, 1249, 1180, 1018, 794 cm^{-1}; HRMS (ESI-TOF, *m/z*): calcd for $C_{15}H_{15}N_2OS$ $[M + H]^+$ 271.0900, found 271.0902.

3-((4-Chlorophenyl)thio)-8-methylimidazo[1,2-a]pyridin-2-ol (29bc).

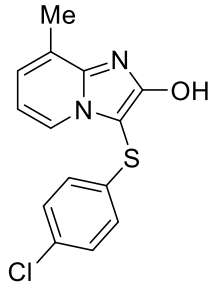

Off-white solid (0.138 g, 94%); MP 238 – 240 °C; ^{1}H NMR (400 MHz, DMSO-d_6) δ 11.88 (bs, 1H), 8.05 (d, J = 6.5 Hz, 1H), 7.36 – 7.29 (m, 2H), 7.25 (d, J = 7.2 Hz, 1H), 7.03 – 6.99 (m, 2H), 6.97 (t, J = 6.8 Hz, 1H), 2.42 (s, 3H); ^{13}C NMR (100 MHz, DMSO-d_6) δ 161.2, 139.4, 136.7, 130.7, 129.6, 127.2, 127.1, 122.0, 114.4, 99.9, 85.9, 16.2; FT-IR ν_{max} (neat) 3564, 3093, 1643, 1612, 1578, 1442, 1318, 1235, 1111, 748 cm^{-1}; HRMS (ESI-TOF, *m/z*): calcd for $C_{14}H_{12}ClN_2OS$ $[M + H]^+$ 291.0353, found 291.0354.

3-((4-Bromophenyl)thio)-8-methylimidazo[1,2-a]pyridin-2-ol (29bd).

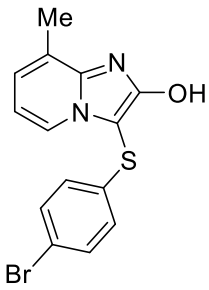

Off-white solid (0.159 g, 95%); MP 246 – 248 °C; ^{1}H NMR (400 MHz, DMSO-d_6) δ 11.88 (bs, 1H), 8.04 (d, J = 6.4 Hz, 1H), 7.45 (d, J = 8.2 Hz, 2H), 7.25 (d, J = 7.2 Hz, 1H), 6.97 (d, J = 6.8 Hz, 1H), 6.94 (d, J = 8.5 Hz, 2H), 2.42 (s, 3H); ^{13}C NMR (100 MHz, DMSO-d_6) δ 161.3, 137.2, 133.6, 132.5, 127.4, 127.1, 122.0, 118.9, 114.4, 99.9, 85.7, 16.2; FT-IR ν_{max} (neat) 3564, 3062, 1620, 1465, 1334, 1249, 1080, 756, 732 cm^{-1}; HRMS (ESI-TOF, *m/z*): calcd for $C_{14}H_{12}BrN_2OS$ $[M + H]^+$ 334.9848, 336.9828, found 334.9820, 336.9799.

3-((4-Nitrophenyl)thio)-8-methylimidazo[1,2-a]pyridin-2-ol (29bg).

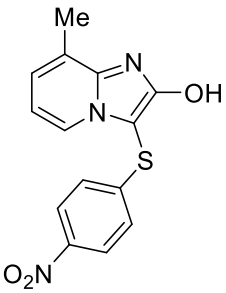

Yellow solid (0.123g, 82%); MP 285 – 287 °C; ^{1}H NMR (400 MHz, DMSO-d_6) δ 12.04 (bs, 1H), 8.19 – 8.08 (m, 2H), 8.05 (d, J = 6.7 Hz, 1H), 7.36 – 7.27 (m, 1H), 7.20 (d, J = 8.2 Hz, 2H), 6.99 (t, J = 7.5 Hz, 1H), 2.43 (s, 2H); ^{13}C NMR (100 MHz, DMSO-d_6) δ 160.8, 148.3, 145.6, 137.3, 130.4, 125.4, 124.8, 124.8, 122.4, 110.3, 83.0, 17.9; FT-IR ν_{max} (neat) 3348, 3070, 2916, 1643, 1604, 1573, 1504, 1374, 1334, 1234, 1080, 840, 740cm^{-1}; HRMS (ESI-TOF, *m/z*): calcd for $C_{14}H_{12}N_3O_3S$ $[M + H]^+$ 302.0594, found 302.0567.

8-Methyl-3-(naphthalen-2-ylthio)imidazo[1,2-a]pyridin-2-ol (29bi).

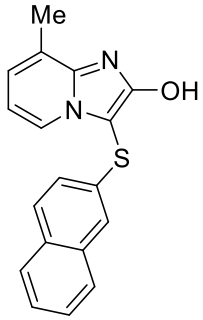

Yellow solid (0.127g, 83%); MP 265 – 267 °C; ^{1}H NMR (400 MHz, DMSO-d_6) δ 11.81 (bs, 1H), 8.08 (d, J = 6.5 Hz, 1H), 7.83 (dd, J = 8.9, 3.9 Hz, 2H), 7.77 – 7.69 (m, 1H), 7.52 (d, J = 1.9 Hz, 1H), 7.44 (pd, J = 7.0, 1.6 Hz, 2H), 7.23 (d, J = 7.2 Hz, 1H), 7.17 (dd, J = 8.6, 1.9 Hz, 1H), 6.94 (t, J = 6.9 Hz, 1H), 2.44 (s, 3H); ^{13}C NMR (100 MHz, DMSO) δ 161.3, 139.5, 135.0, 133.8, 131.7, 129.4, 128.1, 127.3, 127.2, 126.9, 126.0, 124.2, 123.3, 122.01, 121.8, 114.3, 86.5, 16.2; FT-IR ν_{max} (neat) 3363, 3070, 2974, 1612, 1597, 1456, 1313, 1256, 1111, 1072, 782 cm^{-1}; HRMS (ESI-TOF, *m/z*): calcd for $C_{18}H_{15}N_2OS$ $[M + H]^+$ 307.0900, found 307.0878.

3-((4-Chlorophenyl)thio)-7-methylimidazo[1,2-a]pyridin-2-ol (29cc).

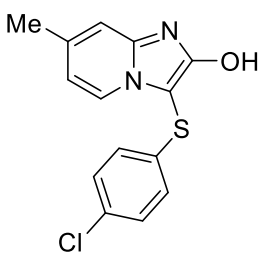

White solid (0.102 g, 71%); MP 244 – 246 °C; ^{1}H NMR (400 MHz, DMSO-d_6) δ 11.82 (bs, 1H), 8.07 (d, J = 6.7 Hz, 1H), 7.33 (d, J = 8.2 Hz, 2H), 7.15 (s, 1H), 7.01 (d, J = 8.1 Hz, 2H), 6.93 (d, J = 6.8 Hz, 1H), 2.38 (s, 3H); ^{13}C NMR (100 MHz, DMSO-d_6) δ 160.8, 139.1, 137.1, 130.5, 129.6, 129.6, 127.0, 123.6, 116.8, 110.1, 83.8, 21.0; FT-IR ν_{max} (neat) 3371, 3047, 2962, 1604, 1597, 1465, 1327, 1265, 1080, 779 cm^{-1}; HRMS (ESI-TOF, *m/z*): calcd for $C_{14}H_{12}ClN_2OS$ $[M + H]^+$ 291.0353, found 291.0338.

3-((4-Bromophenyl)thio)-7-methylimidazo[1,2-a]pyridin-2-ol (29cd).

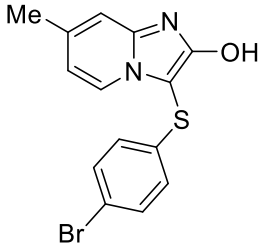

White solid (0.117 g, 70%); MP 246 – 248 °C; ^{1}H NMR (400 MHz, DMSO-d_6) δ 11.78 (bs, 1H), 8.07 (d, J = 6.7 Hz, 1H), 7.62-7.50 (m, 1H), 7.45 (d, J = 8.0 Hz, 2H), 7.14 (s, 1H), 6.94 (d, J = 8.0 Hz, 2H), 2.38 (s, 3H); ^{13}C NMR (100 MHz, DMSO) δ 160.8, 139.1, 137.7, 132.8, 132.4, 129.8, 127.3, 123.6, 118.7, 116.8, 83.7, 21.0; FT-IR ν_{max} (neat) 3365, 3070, 2974, 1643, 1597, 1456, 1313, 1234, 1072, 795 cm^{-1}; HRMS (ESI-TOF, *m/z*): calcd for $C_{14}H_{12}BrN_2OS$ $[M + H]^+$ 334.9848, 336.9828, found 334.9819, 336.9831.

6-Methyl-3-(phenylthio)imidazo[1,2-a]pyridin-2-ol (29da).

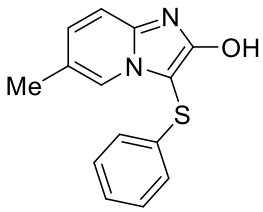

White solid (0.079 g, 62%); MP 248 – 250 °C; ^{1}H NMR (400 MHz, DMSO-d_6) δ 11.68 (bs, 1H), 8.05 (d, J = 1.5 Hz, 1H), 7.27 – 7.22 (m, 4H), 7.17 – 7.10 (m, 1H), 7.02 – 6.95 (m, 2H); ^{13}C NMR (100 MHz, DMSO-d_6) δ 161.0, 137.8, 137.5, 129.7, 129.5, 126.0, 125.3, 124.2, 122.1, 110.9, 85.8, 18.0; FT-IR ν_{max} (neat) 3564, 3055, 1604, 1597, 1465, 165, 1234, 1157, 887, 756 cm^{-1}; HRMS (ESI-TOF, *m/z*): calcd for $C_{14}H_{13}N_2OS$ $[M + H]^+$ 257.0743, found 257.0729.

6-Methyl-3-(p-tolylthio)imidazo[1,2-a]pyridin-2-ol (29db).

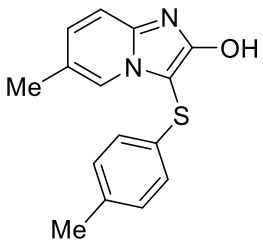

White solid (0.094 g, 70%); MP 221 – 223 °C; ^{1}H NMR (400 MHz, DMSO-d_6) δ 11.66 (bs, 1H), 8.02 (s, 1H), 7.33 – 7.20 (m, 2H), 7.07 (d, J = 7.8 Hz, 2H), 6.91 (d, J = 7.8 Hz, 2H), 2.25 (s, 3H), 2.21 (s, 3H); ^{13}C NMR (100 MHz, DMSO-d_6) δ 165.7, 142.2, 140.2, 138.8, 135.1, 135.1, 134.1, 130.5, 128.8, 126.8, 115.7, 91.1, 25.6, 22.7; FT-IR ν_{max} (neat) 3535, 3363, 1604, 1558, 1465, 1319, 1242, 1111, 884, 756 cm^{-1}; HRMS (ESI-TOF, *m/z*): calcd for $C_{15}H_{15}N_2OS$ [M + H]$^+$ 271.0900, found 271.0884.

3-((4-Chlorophenyl)thio)-6-methylimidazo[1,2-a]pyridin-2-ol (29dc).

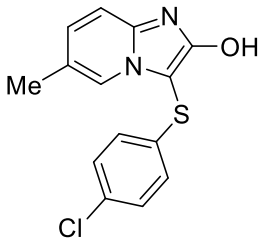

White solid (0.116 g, 80%); MP 232 – 235 °C; ^{1}H NMR (400 MHz, DMSO-d_6) δ 11.73 (bs, 1H), 8.05 (s, 1H), 7.33 (d, J = 8.2 Hz, 2H), 7.28 (d, J = 8.8 Hz, 1H), 7.24 (d, J = 8.8 Hz, 1H), 7.01 (d, J = 8.2 Hz, 2H), 2.27 (s, 3H); ^{13}C NMR (100 MHz, DMSO-d_6) δ 160.9, 137.0, 130.6, 129.8, 129.6, 127.0, 124.4, 122.2, 110.6, 99.6, 85.0, 17.9; FT-IR ν_{max} (neat) 3564, 3387, 3070, 2924, 1643, 1604, 1465, 1319, 1273, 1111, 1080, 894, 740 cm^{-1}; HRMS (ESI-TOF, *m/z*): calcd for $C_{14}H_{12}ClN_2OS$ [M + H]$^+$ 291.0353, found 291.0353.

3-((4-Bromophenyl)thio)-6-methylimidazo[1,2-a]pyridin-2-ol (29dd).

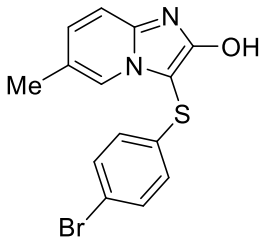

White solid (0.123 g, 74%); MP 248 – 250 °C; ^{1}H NMR (400 MHz, DMSO-d_6) δ 11.84 (bs, 1H), 8.04 (d, J = 1.5 Hz, 1H), 7.51 – 7.38 (m, 2H), 7.33 – 7.17 (m, 2H), 6.99 – 6.87 (m, 2H), 2.27 (s, 3H); ^{13}C NMR (100 MHz, DMSO-d_6) δ 160.9, 137.6, 132.4, 129.8, 127.4, 124.4, 122.2, 118.8, 108.7, 99.9, 89.4, 17.9; FT-IR ν_{max} (neat) 3363, 3070, 2974, 1643, 1597, 1456, 1313, 1234, 1072, 795 cm^{-1}; HRMS (ESI-TOF, *m/z*): calcd for $C_{14}H_{12}BrN_2OS$ [M + H]$^+$ 334.9848, 336.9828, found 334.9852, 336.9831.

6-Methyl-3-((4-nitrophenyl)thio)imidazo[1,2-a]pyridin-2-ol (29dg).

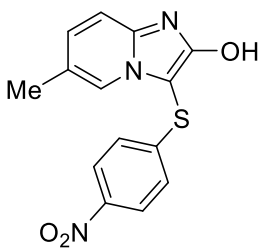

Yellow solid (0.105 g, 70%); MP 275 – 277 °C; ^{1}H NMR (400 MHz, DMSO-d_6) δ 11.84 (bs, 1H), 8.11 (d, J = 8.5 Hz, 2H), 8.05 (s, 1H), 7.36 – 7.28 (m, 1H), 7.27 (d, J = 8.8 Hz, 1H), 7.21 (d, J = 8.7 Hz, 2H), 2.26 (s, 3H); ^{13}C NMR (100 MHz, DMSO) δ 160.8, 148.3, 145.6, 137.3, 130.4, 125.4, 124.8, 124.8, 122.4, 110.3, 83.0, 17.9; FT-IR ν_{max} (neat) 3448, 3070, 2916, 1643, 1604, 1573, 1504, 1334, 1234, 1080, 840, 740, 663 cm^{-1}; HRMS (ESI-TOF, *m/z*): calcd for $C_{14}H_{12}N_3O_3S$ $[M + H]^+$ 302.0594, found 302.0572.

6-Methyl-3-(naphthalen-2-ylthio)imidazo[1,2-a]pyridin-2-ol (29di).

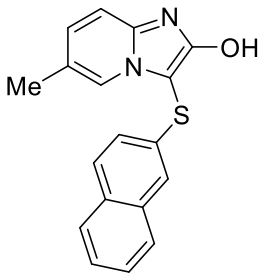

Off-white solid (0.124 g, 81%); MP 245 – 247 °C; ^{1}H NMR (400 MHz, DMSO-d_6) δ 11.77 (bs,1H), 8.08 (s, 1H), 7.84 (dd, J = 8.0, 4.4 Hz, 2H), 7.78 – 7.71 (m, 1H), 7.50 (d, J = 1.8 Hz, 1H), 7.45 (td, J = 7.4, 1.6 Hz, 2H), 7.27 (m, 2H), 7.19 (dd, J = 8.6, 1.9 Hz, 1H), 2.24 (s, 3H) ; ^{13}C NMR (100 MHz, DMSO) δ 161.6, 135.4, 133.8, 131.7, 129.7, 129.4, 128.1, 127.3, 127.2, 125.9, 124.3, 124.1, 122.9, 122.2, 118.7, 115.8, 86.7, 17.9; FT-IR ν_{max} (neat) 3363, 3070, 2974, 1612, 1597, 1456, 1327, 1256, 1180, 1072, 765 cm^{-1}; HRMS (ESI-TOF, *m/z*): calcd for $C_{18}H_{15}N_2OS$ $[M + H]^+$ 307.0900, found 307.0907.

6-Chloro-3-(p-tolylthio)imidazo[1,2-a]pyridin-2-ol (29eb).

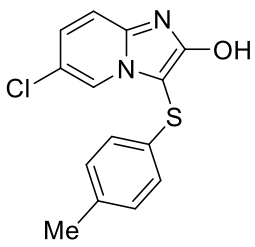

Cream solid (0.117 g, 81%); MP 262 – 264 °C; ^{1}H NMR (400 MHz, DMSO-d_6) δ 11.77 (bs, 1H), 8.26 (s, 1H), 7.42 (s, 2H), 7.09 (d, J = 7.8 Hz, 2H), 6.95 (d, J = 7.8 Hz, 2H), 2.22 (s, 3H); ^{13}C NMR (100 MHz, DMSO-d_6) δ 161.9, 136.0, 132.8, 130.5, 127.0, 126.3, 121.7, 120.6, 116.0, 114.1, 89.7, 20.9; FT-IR ν_{max} (neat) 3364, 3078, 2924, 1612, 1597, 1465, 1303, 1257, 1211, 1180, 1010, 794 cm^{-1}; HRMS (ESI-TOF, *m/z*): calcd for $C_{14}H_{12}ClN_2OS$ $[M + H]^+$ 291.0353, found 291.0357.

6-Bromo-3-(p-tolylthio)imidazo[1,2-a]pyridin-2-ol (29fb).

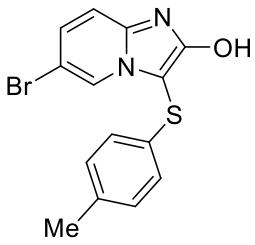

Cream solid (0.135 g, 81%); MP 243 – 245 °C; ^{1}H NMR (400 MHz, DMSO-d_6) δ 11.72 (bs, 1H), 8.29 (s, 1H), 7.50 (d, J = 9.2 Hz, 1H), 7.36 (d, J = 9.4 Hz, 1H), 7.09 (d, J = 7.8 Hz, 2H), 6.94 (d, J = 7.9 Hz, 2H), 2.22 (s, 3H); ^{13}C NMR (100 MHz, DMSO-d_6) δ 161.8, 135.9, 132.8, 130.5, 129.3, 126.3, 123.6, 116.1, 114.3, 107.4, 86.8, 20.9; FT-IR ν_{max} (neat) 3339, 3065, 2919, 1612, 1585, 1465, 1327, 1256, 1180, 1010, 869,794 cm^{-1}; HRMS (ESI-TOF, *m/z*): calcd for $C_{14}H_{12}BrN_2OS$ $[M + H]^+$ 334.9848, 336.9828, found 334.9852, 336.9831.

6-Phenyl-3-(p-tolylthio)imidazo[1,2-a]pyridin-2-ol (29gb).

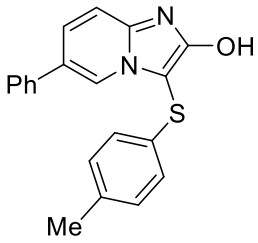

Cream solid (0.132 g, 80%); MP 239 – 241 °C; ^{1}H NMR (400 MHz, DMSO-d_6) δ 11.69 (bs, 1H), 8.29 (s, 1H), 7.71 (d, J = 9.1 Hz, 1H), 7.61 (d, J = 7.6 Hz, 2H), 7.47 (t, J = 8.2 Hz, 3H), 7.40 (d, J = 7.3 Hz, 1H), 7.08 (d, J = 7.8 Hz, 2H), 6.97 (d, J = 7.9 Hz, 2H), 2.20 (s, 3H); ^{13}C NMR (100 MHz, $CDCl_3$) δ 166.3, 141.4, 140.5, 138.2, 135.2, 134.4, 133.2, 132.2, 131.7, 131.2, 130.8, 125.3, 117.2, 92.8, 25.6; FT-IR ν_{max} (neat) 3463, 3070, 2974, 1612, 1597, 1456, 1343, 1227, 1180, 1072, 752 cm^{-1}; HRMS (ESI-TOF, *m/z*): calcd for $C_{20}H_{17}N_2OS$ $[M + H]^+$ 333.1056, found 333.1032.

6-(4-Methoxyphenyl)-3-(phenylthio)imidazo[1,2-a]pyridin-2-ol (29ha).

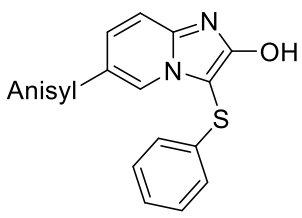

Cream solid (0.104 g, 60%); MP 223 – 225 °C; ^{1}H NMR (400 MHz, DMSO-d_6) δ 8.20 (s, 1H), 7.64 (d, J = 8.8 Hz, 1H), 7.52 (d, J = 8.3 Hz, 2H), 7.41 (d, J = 9.0 Hz, 1H), 7.25 (t, J = 7.6 Hz, 2H), 7.12 (t, J = 7.3 Hz, 1H), 7.02 (t, J = 8.2 Hz, 4H), 3.77 (s, 3H); ^{13}C NMR (100 MHz, DMSO) δ 159.6, 139.0, 137.4, 129.9, 129.7, 129.0, 128.1, 127.9, 127.6, 127.03, 126.1, 125.6, 119.8, 115.0, 114.9, 112.0, 86.9, 55.6 ; FT-IR ν_{max} (neat) 3348, 3093, 1604, 1566, 1473, 1280, 1172, 1018, 740 cm^{-1}; HRMS (ESI-TOF, *m/z*): calcd for $C_{20}H_{17}N_2O_2S$ $[M + H]^+$ 349.1005, found 349.1012.

6-(4-Methoxyphenyl)-3-(p-tolylthio)imidazo[1,2-a]pyridin-2-ol (29hb).

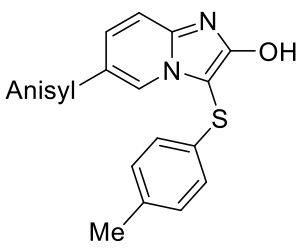

Cream solid (0.123 g, 68%); MP 239 – 241 °C; ^{1}H NMR (400 MHz, DMSO-d_6) δ 11.84 (bs, 1H), 8.21 (s, 1H), 7.66 (d, J = 8.9 Hz, 1H), 7.53 (d, J = 8.3 Hz, 2H), 7.41 (d, J = 9.1 Hz, 1H), 7.07 (d, J = 8.0 Hz, 2H), 7.02 (d, J = 8.3 Hz, 2H), 6.96 (d, J = 8.0 Hz, 2H), 3.78 (s, 3H), 2.20 (s, 3H); ^{13}C NMR (100 MHz, DMSO-d_6) δ 161.4, 159.7, 138.7, 135.7, 133.5, 130.4, 128.9, 128.2, 127.3, 126.3, 126.0, 119.9, 115.1, 106.4, 87.8, 55.7, 20.9; FT-IR ν_{max} (neat) 3564, 3362, 2916, 1635, 1604, 1489, 1319, 1242, 1172, 1018, 802, 748 cm^{-1}; HRMS (ESI-TOF, *m/z*): calcd for $C_{21}H_{19}N_2O_2S$ $[M + H]^+$ 363.1162, found 363.1163.

3-((4-Chlorophenyl)thio)-6-(4-methoxyphenyl)imidazo[1,2-a]pyridin-2-ol (29hc).

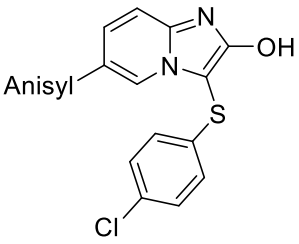

White solid (0.159 g, 83%); MP 255 – 257 °C; ^{1}H NMR (400 MHz, DMSO-d_6) δ 11.82 (bs, 1H), 8.24 (s, 1H), 7.69 (dd, J = 9.0, 1.9 Hz, 1H), 7.55 (d, J = 8.3 Hz, 2H), 7.42 (d, J = 9.0 Hz, 1H), 7.32 (d, J = 8.2 Hz, 2H), 7.06 (d, J = 8.3 Hz, 2H), 7.02 (d, J = 8.3 Hz, 2H), 3.78 (s, 3H); ^{13}C NMR (100 MHz, DMSO-d_6) δ 161.3, 159.7, 136.5, 134.9, 130.7, 129.6, 128.8, 128.2, 127.6, 127.3, 126.7, 120.0, 115.1, 111.8, 86.4, 55.7; FT-IR ν_{max} (neat) 3356, 2924, 1635, 1496, 1465, 1319, 1242, 1211, 1080, 802 cm^{-1}; HRMS (ESI-TOF, *m/z*): calcd for $C_{20}H_{16}ClN_2O_2S$ $[M + H]^+$ 383.0616, found 383.0617.

1,2-Di-p-tolyldisulfane (32).

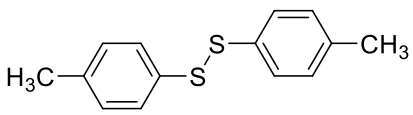

White solid (0.183 g, 92%); MP 45 – 47 °C; ^{1}H NMR (400 MHz, $CDCl_3$-*d*) δ 7.64 – 7.30 (m, 4H), 7.15 (d, J = 8.0 Hz, 4H), 2.36 (s, 6H); ^{13}C NMR (100 MHz, $CDCl_3$) δ 137.4, 133.9, 129.8, 128.5, 21.1; HRMS (ESI-TOF, *m/z*): calcd for $C_{14}H_{15}S_2$ $[M + H]^+$ 247.0610, found 247.0598.

5.4.3 General Procedure for the Synthesis of 2-aryl-3-sulfenylimidazo[1,2-*a*]pyridine (31a-31c)

An oven-dried 10 mL round bottom flask was charged with 3-(*p*-tolylthio)imidazo[1,2-*a*]pyridin-2-ol (0.500 g, 1.95 mmol) and dichloromethane (15 mL). The resulting solution was stirred and

cooled to 0 °C before adding sequentially triethylamine (0.295 g, 2.92 mmol) and *p*-toluenesulfonyl chloride (0.556 g, 2.95 mmol) drop wise and portion wise. The resulting solution was stirred at 0 °C until TLC showed complete consumption of starting material. The resulting suspension was diluted with dichloromethane (50 mL), stirred for a further 30 minutes and the precipitate removed by filtration. The solution was then washed sequentially with 10% aqueous sodium hydrogen carbonate (2 x 15 mL) and a saturated aqueous sodium chloride solution (30 mL). The combined organic layers were dried over magnesium sulfate, filtered, and concentrated in *vacuo* to obtain crude tosylated product (0.430 g, 56 %). The 10 mL round bottom flask was charged with crude tosylated product (0.100 g, 0.25 mmol), phenyl boronic (0.046 g, 0.38 mmol) and K_3PO_4 (0.134 g, 0.63 mmol) and $Pd(OAc)_2$ (0.001 g, 2 mol %) in ethylene glycol (5 mL). To the resulting solution was stirred at 80 °C under air until TLC showed complete consumption of tosylated product. After completion of the reaction, the mixture was poured into water, extracted by ethyl acetate, washed with brine and dried with anhydrous Na_2SO_4. The organic solvent was removed under reduced pressure to obtain crude product. The crude residue was subjected to column chromatography (EtOAc : hexane; 3:7 *v/v*) to afford **31a** in (0.050 g, 63 %) yield as yellow colored solid.

2-Phenyl-3-(p-tolylthio)imidazo[1,2-a]pyridine (31a).

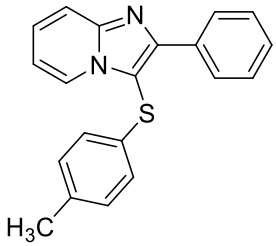

Yellow solid (0.050 g, 63%); ^{1}H NMR (400 MHz, $CDCl_3$) δ 8.30 (dt, J = 6.8, 1.2 Hz, 1H), 8.29 – 8.20 (m, 2H), 7.75 (dt, J = 8.9, 1.1 Hz, 1H), 7.50 – 7.44 (m, 2H), 7.45 – 7.35 (m, 1H), 7.35 (ddd, J = 9.0, 6.8, 1.3 Hz, 1H), 7.09 – 7.00 (m, 2H), 6.98 – 6.90 (m, 2H), 6.88 (td, J = 6.8, 1.2 Hz, 1H), 2.28 (s, 3H); ^{13}C NMR (100 MHz, $CDCl_3$) δ 146.44, 142.27, 131.30, 128.67, 126.75, 125.47, 123.81, 123.67, 123.64, 122.76, 121.84, 121.08, 119.79, 112.87, 108.27, 102.13, 16.15; HRMS (ESI-TOF, *m/z*): calcd for $C_{20}H_{17}N_2S$ $[M + H]^+$ 317.1107, found 317.1120.

2-(p-Tolyl)-3-(p-tolylthio)imidazo[1,2-a]pyridine (31b).

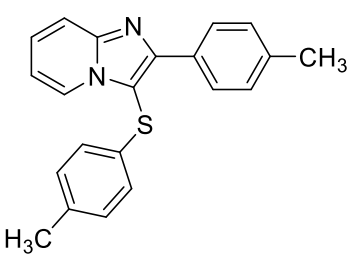

Yellow solid (0.040 g, 48%); ^{1}H NMR (400 MHz, $CDCl_3$) δ 8.29 (dt, J = 6.8, 1.2 Hz, 1H), 8.19 – 8.06 (m, 2H), 7.74 (dt, J = 9.0, 1.2 Hz, 1H), 7.34 (ddd, J = 8.6, 6.9, 1.4 Hz, 1H), 7.27 (d, J = 8.5 Hz, 2H), 7.04 (d, J = 8.1 Hz, 2H), 6.98 – 6.90 (m, 2H), 6.89 – 6.83 (m, 1H), 2.41 (s, 3H), 2.28 (s, 3H); ^{13}C NMR (100 MHz, $CDCl_3$) δ 151.2, 146.95, 138.5, 135.9, 131.5, 130.4, 130.1, 129.1, 128.2, 126.5, 125.8, 124.5, 117.4, 112.9, 106.5, 21.3, 20.9; HRMS (ESI-TOF, *m/z*): calcd for $C_{21}H_{19}N_2S$ $[M + H]^+$ 331.1263, found 331.1249.

2-(4-Chlorophenyl)-3-(p-tolylthio)imidazo[1,2-a]pyridine (31c).

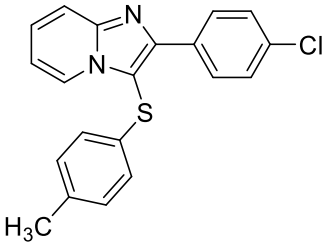

White solid (0.070g, 79%); ^{1}H NMR (400 MHz, $CDCl_3$) δ 8.29 (d, J = 6.9 Hz, 1H), 8.21 (d, J = 8.6 Hz, 2H), 7.73 (d, J = 9.0 Hz, 1H), 7.42 (d, J = 8.6 Hz, 2H), 7.34 (ddd, J = 8.7, 6.8, 1.3 Hz, 1H), 7.03 (d, J = 8.0 Hz, 2H), 6.91 (d, J = 8.2 Hz, 2H), 6.87 (d, J = 6.9 Hz, 1H), 2.27 (s, 3H); ^{13}C NMR (100 MHz, $CDCl_3$) δ 149.8, 146.9, 136.2, 134.5, 131.8, 131.1, 130.3, 129.6, 128.6, 126.9, 125.8, 124.5, 117.5, 113.2, 107.1, 20.92; HRMS (ESI-TOF, *m/z*): calcd for $C_{20}H_{16}ClN_2S$ $[M + H]^+$ 351.0717, found 351.0725.

5.4.4 Single X-ray Analysis of 3-((4-Bromophenyl)thio)imidazo[1,2-*a*]pyridin-2-ol (29ad)

5.4.4.1 Experimental

Single crystals of $C_{13}H_9BrN_2OS$ **(29ad)** were generated. A suitable crystal was selected and analyzed on XtaLAB Pro: Kappa dual offset/far diffractometer. The crystal was kept at 93(2) K during data collection. Using Olex2,[64] the structure was solved with the ShelXT[65] structure solution program using Intrinsic Phasing and refined with the ShelXL[66] refinement package using Least Squares minimization.

Crystal Data for $C_{13}H_9BrN_2OS$ (M =321.19 g/mol): monoclinic, space group Cc (no. 9), a = 27.5712(12) Å, b = 5.3813(3) Å, c = 16.6101(9) Å, β = 94.187(4)°, V = 2457.8(2) Å^3, Z = 8, T = 93(2) K, μ(MoKα) = 3.502 mm^{-1}, *Dcalc* = 1.736 g/cm^3, 10424 reflections measured (7.422° ≤ 2Θ ≤ 59.386°), 5106 unique (R_{int} = 0.0196, R_{sigma} = 0.0289) which were used in all calculations. The final R_1 was 0.0298 (I > 2σ(I)) and wR_2 was 0.0777 (all data).

Refinement Model Description

Number of restraints - 2, number of constraints - unknown.

Details:

1. Fixed Uiso At 1.2 times of: All C(H) groups, All N(H) groups
2. Aromatic/amide H refined with riding coordinates: N2A(H2A), N2(H2), C9(H9), C1(H1), C1A(H1A), C3(H3), C12(H12), C9A(H9A), C10(H10), C2(H2B), C3A(H3A), C12A(H12A), C4A(H4A), C2A(H2AA), C4(H4), C13(H13), C10A(H10A), C13A(H13A)

Table 5.3 Crystal data and structure refinement for **29ad**

Identification code	exp_247-KP-916
Empirical formula	$C_{13}H_9BrN_2OS$
Formula weight	321.19
Temperature/K	93(2)
Crystal system	monoclinic
Space group	Cc
a/Å	27.5712(12)
b/Å	5.3813(3)
c/Å	16.6101(9)
α/°	90
β/°	94.187(4)
γ/°	90
Volume/Å^3	2457.8(2)
Z	8
ρ_{calc}g/cm^3	1.736
μ/mm^{-1}	3.502

F(000)	1280.0
Crystal size/mm^3	0.3 × 0.1 × 0.05
Radiation	MoKα (λ = 0.71073)
2Θ range for data collection/°	7.422 to 59.386
Index ranges	-34 ≤ h ≤ 37, -6 ≤ k ≤ 7, -21 ≤ l ≤ 22
Reflections collected	10424
Independent reflections	5106 [R_{int} = 0.0196, R_{sigma} = 0.0289]
Data/restraints/parameters	5106/2/325
Goodness-of-fit on F^2	1.067
Final R indexes [I>=2σ (I)]	R_1 = 0.0298, wR_2 = 0.0762
Final R indexes [all data]	R_1 = 0.0331, wR_2 = 0.0777
Largest diff. peak/hole / e Å^{-3}	0.40/-0.35

Table 5.4 Fractional Atomic Coordinates (×10^4) and Equivalent Isotropic Displacement Parameters (Å^2×10^3) for **29ad**. U_{eq} is defined as 1/3 of of the trace of the orthogonalised U_{IJ} tensor**.**

Atom	*x*	*y*	*Z*	U(eq)
Br1A	1840.1(2)	5473.4(9)	3193.6(3)	26.32(13)
Br1	8160.0(2)	-297.1(9)	6247.2(3)	27.01(13)
S1A	3973.5(4)	9670.5(19)	4354.5(7)	18.2(2)
S1	5975.4(4)	-4589.5(19)	5683.4(6)	16.5(2)
O1	5237.4(12)	345(6)	5800(2)	18.7(6)
O1A	4691.9(13)	4622(6)	4218(2)	19.0(7)
N1A	4214.2(13)	7650(6)	5844(2)	14.7(7)
N2A	4674.3(14)	4422(7)	5622(2)	16.2(7)
N1	5721.0(13)	-2694(6)	4174(2)	13.6(7)
N2	5260.6(14)	553(7)	4395(2)	15.4(7)

C9	6713.1(17)	-1175(9)	5445(3)	20.1(9)
C8	6576.7(15)	-3353(7)	5825(3)	15.2(8)
C1	5959.9(15)	-4371(8)	3731(3)	16.2(8)
C1A	3989.3(18)	9374(8)	6288(3)	16.5(9)
C3	5687.6(16)	-2125(8)	2525(3)	17.4(8)
C5A	4481.3(16)	5761(8)	6209(3)	14.5(8)
C12	7393.4(17)	-3775(8)	6458(3)	21.1(9)
C11A	2464.5(17)	6726(8)	3550(3)	20.0(9)
C11	7518.8(16)	-1610(8)	6075(3)	18.7(9)
C9A	3330.9(18)	6245(9)	3639(3)	22.4(9)
C6A	4543.5(16)	5457(8)	4860(3)	15.2(8)
C7A	4238.7(16)	7486(8)	5003(3)	15.3(8)
C10	7191.1(17)	-308(8)	5574(3)	20.7(9)
C8A	3379.1(15)	8425(8)	4078(3)	16.9(8)
C2	5944.2(18)	-4122(8)	2910(3)	18.4(9)
C3A	4289.9(16)	7246(8)	7500(3)	17.4(8)
C7	5686.2(15)	-2553(8)	5013(3)	15.9(8)
C6	5386.2(16)	-500(8)	5159(3)	15.9(9)
C12A	2504.8(17)	8922(9)	3982(3)	23.4(9)
C4A	4518.5(16)	5504(8)	7050(3)	16.8(8)
C2A	4027.6(17)	9191(8)	7116(3)	18.2(8)
C4	5445.0(16)	-448(8)	2975(3)	15.5(8)
C13	6917.3(17)	-4645(7)	6331(3)	18.8(8)
C5	5458.5(15)	-760(8)	3807(3)	14.3(8)
C10A	2872.1(18)	5377(8)	3367(3)	22.9(9)

C13A	2969.6(18)	9763(8)	4261(3)	21.3(9)

Table 5.5 Anisotropic Displacement Parameters ($Å^2×10^3$) for **29ad**. The Anisotropic displacement factor exponent takes the form: $-2\pi^2[h^2a^{*2}U_{11}+2hka^*b^*U_{12}+\ldots]$.

Atom	**U_{11}**	**U_{22}**	**U_{33}**	**U_{23}**	**U_{13}**	**U_{12}**
Br1A	17.9(2)	30.5(2)	29.7(3)	6.3(2)	-4.24(18)	-5.2(2)
Br1	14.7(2)	28.5(2)	37.4(3)	-3.5(3)	-1.16(19)	-3.8(2)
S1A	21.1(5)	20.0(4)	13.2(5)	3.7(4)	-1.5(4)	-6.8(4)
S1	17.0(5)	19.4(4)	13.0(5)	2.8(4)	-0.7(4)	-5.2(4)
O1	18.6(15)	24.1(15)	13.3(16)	-5.0(12)	1.8(12)	-3.0(12)
O1A	20.7(17)	25.6(17)	10.9(16)	-1.7(12)	2.2(12)	-3.2(13)
N1A	13.8(16)	19.3(16)	10.9(18)	0.6(13)	-0.5(12)	-5.0(13)
N2A	15.6(17)	18.6(17)	15(2)	-2.4(13)	1.4(13)	-1.4(13)
N1	12.6(17)	17.1(16)	11.0(18)	0.3(12)	0.3(13)	-3.1(12)
N2	17.4(18)	18.3(17)	10.4(18)	-0.7(13)	0.4(13)	-0.4(13)
C9	19(2)	22(2)	19(2)	5.8(17)	-1.8(17)	-1.3(17)
C8	17.2(19)	16.0(18)	12.2(19)	-3.0(15)	0.0(14)	-3.1(15)
C1	16(2)	17.3(18)	15(2)	-1.4(15)	-0.1(15)	-0.4(15)
C1A	20(2)	14.2(18)	15(2)	0.6(15)	3.1(17)	-0.7(16)
C3	18(2)	23(2)	10(2)	0.4(16)	0.0(15)	-1.7(16)
C5A	13(2)	17.1(18)	13(2)	-0.4(15)	1.7(15)	-3.0(15)
C12	21(2)	21(2)	21(2)	1.3(17)	-2.5(16)	2.5(17)
C11A	18(2)	23(2)	19(2)	8.1(17)	-2.2(16)	-3.8(17)
C11	11(2)	20.6(19)	24(2)	-4.1(17)	2.1(16)	-1.8(16)
C9A	19(2)	23(2)	25(2)	-2.4(19)	-0.2(18)	3.1(17)
C6A	16(2)	19.6(19)	10(2)	-1.6(15)	-0.5(15)	-7.3(16)

C7A	16(2)	18.6(19)	11(2)	1.2(15)	-0.4(15)	-2.2(15)
C10	22(2)	19.2(19)	21(2)	2.7(17)	-0.5(17)	-6.9(16)
C8A	17(2)	19.8(19)	13(2)	3.4(15)	-0.9(15)	-2.9(15)
C2	20(2)	20.6(19)	15(2)	-1.9(17)	4.3(17)	-1.5(17)
C3A	19(2)	23.1(19)	11(2)	-0.5(15)	3.9(15)	-4.3(15)
C7	15(2)	20.8(19)	12(2)	-2.1(15)	1.8(14)	-4.3(15)
C6	9.8(19)	22(2)	15(2)	0.4(16)	-2.9(15)	-5.7(15)
C12A	19(2)	23(2)	29(3)	0.9(19)	2.8(18)	2.0(17)
C4A	17(2)	19.0(19)	14(2)	1.8(15)	2.6(16)	-1.3(16)
C2A	18(2)	20(2)	17(2)	-2.7(16)	4.4(16)	-1.8(16)
C4	12.7(19)	17.9(19)	15(2)	2.4(15)	-2.3(16)	-2.6(15)
C13	22(2)	14.9(17)	19(2)	1.3(15)	1.6(16)	0.8(15)
C5	10.6(18)	16.0(19)	16(2)	-0.8(15)	-1.2(14)	-2.2(14)
C10A	24(2)	21(2)	23(2)	-2.4(17)	-1.6(18)	-2.3(17)
C13A	26(2)	16.6(18)	21(2)	-1.1(16)	3.0(18)	-1.0(16)

Table 5.6 Bond Lengths for **29ad**.

Atom	**Atom**	**Length/Å**	**Atom**	**Atom**	**Length/Å**
Br1A	C11A	1.903(5)	C8	C13	1.398(6)
Br1	C11	1.906(4)	C1	C2	1.368(6)
S1A	C7A	1.721(4)	C1A	C2A	1.374(7)
S1A	C8A	1.799(4)	C3	C2	1.413(6)
S1	C8	1.786(4)	C3	C4	1.376(6)
S1	C7	1.717(4)	C5A	C4A	1.401(6)
O1	C6	1.255(6)	C12	C11	1.383(6)

O1A	C6A	1.254(6)	C12	C13	1.395(6)
N1A	C1A	1.363(6)	C11A	C12A	1.382(7)
N1A	C5A	1.370(6)	C11A	C10A	1.390(7)
N1A	C7A	1.407(5)	C11	C10	1.376(7)
N2A	C5A	1.352(5)	C9A	C8A	1.383(6)
N2A	C6A	1.406(6)	C9A	C10A	1.392(7)
N1	C1	1.364(5)	C6A	C7A	1.409(6)
N1	C7	1.407(5)	C8A	C13A	1.391(6)
N1	C5	1.383(5)	C3A	C4A	1.379(6)
N2	C6	1.410(6)	C3A	C2A	1.399(6)
N2	C5	1.352(5)	C7	C6	1.412(6)
C9	C8	1.396(6)	C12A	C13A	1.405(7)
C9	C10	1.400(6)	C4	C5	1.390(6)

Table 5.7 Bond Angles for **29ad**.

Atom	**Atom**	**Atom**	**Angle/°**	**Atom**	**Atom**	**Atom**	**Angle/°**
C7A	S1A	C8A	104.1(2)	O1A	C6A	N2A	123.1(4)
C7	S1	C8	103.3(2)	O1A	C6A	C7A	131.1(4)
C1A	N1A	C5A	121.2(4)	N2A	C6A	C7A	105.8(4)
C1A	N1A	C7A	129.6(4)	N1A	C7A	S1A	122.0(3)
C5A	N1A	C7A	109.2(3)	N1A	C7A	C6A	106.7(4)
C5A	N2A	C6A	110.4(4)	C6A	C7A	S1A	131.0(3)
C1	N1	C7	129.9(4)	C11	C10	C9	119.5(4)
C1	N1	C5	121.2(4)	C9A	C8A	S1A	120.1(3)
C5	N1	C7	108.9(3)	C9A	C8A	C13A	120.4(4)

C5	N2	C6	110.8(4)	C13A	C8A	S1A	119.4(3)
C8	C9	C10	119.5(4)	C1	C2	C3	120.2(4)
C9	C8	S1	122.1(3)	C4A	C3A	C2A	120.2(4)
C9	C8	C13	119.8(4)	N1	C7	S1	123.1(3)
C13	C8	S1	118.1(3)	N1	C7	C6	107.2(4)
N1	C1	C2	119.5(4)	C6	C7	S1	129.7(4)
N1A	C1A	C2A	119.2(4)	O1	C6	N2	123.0(4)
C4	C3	C2	120.1(4)	O1	C6	C7	131.4(4)
N1A	C5A	C4A	120.8(4)	N2	C6	C7	105.6(4)
N2A	C5A	N1A	107.8(4)	C11A	C12A	C13A	118.9(4)
N2A	C5A	C4A	131.5(4)	C3A	C4A	C5A	118.0(4)
C11	C12	C13	118.5(4)	C1A	C2A	C3A	120.6(4)
C12A	C11A	Br1A	120.1(4)	C3	C4	C5	118.8(4)
C12A	C11A	C10A	121.6(4)	C12	C13	C8	120.5(4)
C10A	C11A	Br1A	118.3(4)	N1	C5	C4	120.2(4)
C12	C11	Br1	120.3(4)	N2	C5	N1	107.5(4)
C10	C11	Br1	117.6(3)	N2	C5	C4	132.2(4)
C10	C11	C12	122.2(4)	C11A	C10A	C9A	118.9(4)
C8A	C9A	C10A	120.4(4)	C8A	C13A	C12A	119.8(4)

Table 5.8 Hydrogen Bonds for **29ad**.

D	**H**	**A**	**d(D-H)/Å**	**d(H-A)/Å**	**d(D-A)/Å**	**D-H-A/°**
N2A	H2A	O1	0.86	1.83	2.691(5)	175.9
N2	H2	O1A	0.86	1.84	2.697(5)	175.8

Table 5.9 Hydrogen Atom Coordinates ($Å \times 10^4$) and Isotropic Displacement Parameters ($Å^2 \times 10^3$) for **29ad**.

Atom	***x***	***Y***	***z***	**U(eq)**
H2A	4852.06	3119.81	5703.94	19
H2	5082.31	1853.06	4313.61	18
H9	6488.01	-306.19	5108.93	24
H1	6132.08	-5672.26	3984.88	19
H1A	3811.97	10659.54	6034.69	20
H3	5682.84	-1944.82	1967.9	21
H12	7621.32	-4632.48	6791.83	25
H9A	3606.52	5354.39	3523.93	27
H10	7286.32	1137.5	5321.73	25
H2B	6102.82	-5271.64	2603.52	22
H3A	4310.21	7126.97	8059.68	21
H12A	2228.97	9827.13	4086.18	28
H4A	4692.14	4196.76	7298.08	20
H2AA	3877.81	10370.17	7423.3	22
H4	5275.1	870.19	2726.37	19
H13	6825.88	-6095.2	6584.01	23
H10A	2838.84	3918.38	3067.93	28
H13A	3003.25	11209.14	4566.38	26

5.5 REFERENCES

[1] H. Guo, B. Sun, H. Gao, X. Chen, S. Liu, X. Yao, X. Liu, Y. Che, *Journal of Natural Products* **2009**, *72*, 2115-2119.

[2] J.-M. Wang, G.-Z. Ding, L. Fang, J.-G. Dai, S.-S. Yu, Y.-H. Wang, X.-G. Chen, S.-G. Ma, J. Qu, S. Xu, D. Du, *Journal of Natural Products* **2010**, *73*, 1240-1249.

[3] P. J. Knerr, A. Tzekou, D. Ricklin, H. Qu, H. Chen, W. A. van der Donk, J. D. Lambris, *ACS Chemical Biology* **2011**, *6*, 753-760.

[4] G. Liu, J. R. Huth, E. T. Olejniczak, R. Mendoza, P. DeVries, S. Leitza, E. B. Reilly, G. F. Okasinski, S. W. Fesik, T. W. von Geldern, *Journal of Medicinal Chemistry* **2001**, *44*, 1202-1210.

[5] M. Feng, B. Tang, S. H. Liang, X. Jiang, *Current topics in medicinal chemistry* **2016**, *16*, 1200-1216.

[6] C. Madaan, S. Saraf, G. Priyadarshani, P. P. Reddy, S. K. Guchhait, A. C. Kunwar, B. Sridhar, *Synlett* **2012**, *23*, 1955-1959.

[7] T. Kondo, T.-a. Mitsudo, *Chemical Reviews* **2000**, *100*, 3205-3220.

[8] P. Chauhan, S. Mahajan, D. Enders, *Chemical Reviews* **2014**, *114*, 8807-8864.

[9] M. Jereb, A. Togni, *Organic Letters* **2005**, *7*, 4041-4043.

[10] M. Chen, Z.-T. Huang, Q.-Y. Zheng, *Chemical Communications* **2012**, *48*, 11686-11688.

[11] J. Li, C. Li, S. Yang, Y. An, W. Wu, H. Jiang, *The Journal of Organic Chemistry* **2016**, *81*, 7771-7783.

[12] F.-J. Chen, G. Liao, X. Li, J. Wu, B.-F. Shi, *Organic Letters* **2014**, *16*, 5644-5647.

[13] Z. Zhou, Y. Liu, J. Chen, E. Yao, J. Cheng, *Organic Letters* **2016**, *18*, 5268-5271.

[14] G. S. A., K. Thomas, L. Chao-Jun, *Angewandte Chemie International Edition* **2014**, *53*, 74-100.

[15] W.-J. Yoo, C.-J. Li, in *C-H Activation* (Eds.: J.-Q. Yu, Z. Shi), Springer Berlin Heidelberg, Berlin, Heidelberg, **2010**, pp. 281-302.

[16] B. V. Varun, J. Dhineshkumar, K. R. Bettadapur, Y. Siddaraju, K. Alagiri, K. R. Prabhu, *Tetrahedron Letters* **2017**, *58*, 803-824.

[17] C. Liu, D. Liu, A. Lei, *Accounts of Chemical Research* **2014**, *47*, 3459-3470.

[18] Y. Wu, J. Wang, F. Mao, F. Y. Kwong, *Chemistry – An Asian Journal* **2014**, *9*, 26-47.

[19] C.-L. Sun, Z.-J. Shi, *Chemical Reviews* **2014**, *114*, 9219-9280.

[20] J. Bariwal, E. Van der Eycken, *Chemical Society Reviews* **2013**, *42*, 9283-9303.

[21] J. A. Rodriguez, J. Hrbek, *Accounts of Chemical Research* **1999**, *32*, 719-728.

[22] J. S. Yadav, B. V. Subba Reddy, R. Jain, G. Baishya, *Tetrahedron Letters* **2008**, *49*, 3015-3018.

[23] B. V. Varun, K. Gadde, K. R. Prabhu, *Organic Letters* **2015**, *17*, 2944-2947.

[24] B. V. Varun, K. Gadde, K. R. Prabhu, *Organic & Biomolecular Chemistry* **2016**, *14*, 7665-7670.

[25] Y. Siddaraju, K. R. Prabhu, *Organic Letters* **2016**, *18*, 6090-6093.

[26] Y. Siddaraju, K. R. Prabhu, *The Journal of Organic Chemistry* **2018**, *83*, 2986-2992.

[27] H. Cao, J. Yuan, C. Liu, X. Hu, A. Lei, *RSC Advances* **2015**, *5*, 41493-41496.

[28] Q. Chen, X. Wang, C. Wen, Y. Huang, X. Yan, J. Zeng, *RSC Advances* **2017**, *7*, 39758-39761.

[29] X. Liu, H. Cui, D. Yang, S. Dai, T. Zhang, J. Sun, W. Wei, H. Wang, *RSC Advances* **2016**, *6*, 51830-51833.

[30] R. D. Kamani, V. B. Purohit, R. P. Thummar, N. H. Sapariya, B. K. Vaghasiya, K. H. Patel, C. T. Pashavan, M. K. Shah, D. K. Raval, *ChemistrySelect* **2017**, *2*, 9670-9673.

[31] Y. Siddaraju, K. R. Prabhu, *Organic & Biomolecular Chemistry* **2017**, *15*, 5191-5196.

[32] C. J. Nalbandian, E. M. Miller, S. T. Toenjes, J. L. Gustafson, *Chemical Communications* **2017**, *53*, 1494-1497.

[33] L. A. G., E. Danish, Saima, S. A. K., *Advanced Synthesis & Catalysis* **2018**, *360*, 180-185.

[34] W. Guo, W. Tan, M. Zhao, K. Tao, L.-Y. Zheng, Y. Wu, D. Chen, X.-L. Fan, *RSC Advances* **2017**, *7*, 37739-37742.

[35] F. Bai, S. Zhang, L. Wei, Y. Liu, *Asian Journal of Organic Chemistry* **2018**, *7*, 371-373.

[36] B. Li, Z. Chen, H. Cao, H. Zhao, *Organic Letters* **2018**, *20*, 3291-3295.

[37] D. Yang, P. Sun, W. Wei, L. Meng, L. He, B. Fang, W. Jiang, H. Wang, *Organic Chemistry Frontiers* **2016**, *3*, 1457-1461.

[38] A. Heidari, *J Data Mining Genomics & Proteomics* **2016**, *7*, e125.

[39] A. Deep, R. Kaur Bhatia, R. Kaur, S. Kumar, U. Kumar Jain, H. Singh, S. Batra, D. Kaushik, P. Kishore Deb, *Current Topics in Medicinal Chemistry* **2017**, *17*, 238-250.

[40] C. Enguehard-Gueiffier, A. Gueiffier, *Mini Reviews in Medicinal Chemistry* **2007**, *7*, 888-899.

[41] J. G. Lombardino, *Journal of Medicinal Chemistry* **1981**, *24*, 39-42.

[42] J. Jiao, L. Wei, X. M. Ji, M. L. Hu, R. Y. Tang, *Advanced Synthesis & Catalysis* **2016**, *358*, 268-275.

[43] D.-Q. Dong, S.-H. Hao, D.-S. Yang, L.-X. Li, Z.-L. Wang, *European Journal of Organic Chemistry* **2017**, *2017*, 6576-6592.

[44] C. Ravi, S. Adimurthy, *The Chemical Record* **2017**, *17*, 1019-1038.

[45] C. Ravi, D. Chandra Mohan, S. Adimurthy, *Organic & Biomolecular Chemistry* **2016**, *14*, 2282-2290.

[46] C. Ravi, A. Joshi, S. Adimurthy, *European Journal of Organic Chemistry* **2017**, *2017*, 3646-3651.

[47] B. Du, B. Jin, P. Sun, *Organic Letters* **2014**, *16*, 3032-3035.

[48] W. Ge, X. Zhu, Y. Wei, *European Journal of Organic Chemistry* **2013**, *2013*, 6015-6020.

[49] S. M. Patil, S. Kulkarni, M. Mascarenhas, R. Sharma, S. M. Roopan, A. Roychowdhury, *Tetrahedron* **2013**, *69*, 8255-8262.

[50] J. Rafique, S. Saba, A. R. Rosário, A. L. Braga, *Chemistry – A European Journal* **2016**, *22*, 11854-11862.

[51] M.-A. Hiebel, S. Berteina-Raboin, *Green Chemistry* **2015**, *17*, 937-944.

[52] C. Ravi, N. N. K. Reddy, V. Pappula, S. Samanta, S. Adimurthy, *The Journal of Organic Chemistry* **2016**, *81*, 9964-9972.

[53] D. C. Mohan, S. N. Rao, C. Ravi, S. Adimurthy, *Asian Journal of Organic Chemistry* **2014**, *3*, 609-613.

[54] C. Ravi, D. Chandra Mohan, S. Adimurthy, *Organic Letters* **2014**, *16*, 2978-2981.

[55] Y. Siddaraju, K. R. Prabhu, *The Journal of Organic Chemistry* **2016**, *81*, 7838-7846.

[56] H. Iida, R. Demizu, R. Ohkado, *The Journal of Organic Chemistry* **2018**.

[57] R. Rahaman, S. Das, P. Barman, *Green Chemistry* **2018**, *20*, 141-147.

[58] S. Wang, K. Fang, G. Dong, S. Chen, N. Liu, Z. Miao, J. Yao, J. Li, W. Zhang, C. Sheng, *Journal of Medicinal Chemistry* **2015**, *58*, 6678-6696.

[59] K. C. Nicolaou, C. R. H. Hale, C. Nilewski, H. A. Ioannidou, *Chemical Society Reviews* **2012**, *41*, 5185-5238.

[60] N. K. C., N. A. L., M. R. R., S. C. S., *Angewandte Chemie International Edition* **2006**, *45*, 6527-6532.

[61] K. Pandey, P. Kaswan, Saroj, A. Kumar, *ChemistrySelect* **2016**, *1*, 6669-6672.

[62] K. Pandey, K. Rangan, A. Kumar, *The Journal of Organic Chemistry* **2018**, *83*, 8026-8035.

[63] F.-C. Jia, C. Xu, Z.-W. Zhou, Q. Cai, Y.-D. Wu, A.-X. Wu, *Organic Letters* **2016**, *18*, 5232-5235.

[64] O. V. Dolomanov, L. J. Bourhis, R. J. Gildea, J. A. K. Howard, H. Puschmann, *Journal of Applied Crystallography* **2009**, *42*, 339-341.

[65] G. Sheldrick, *Acta Crystallographica Section A* **2015**, *71*, 3-8.

[66] G. Sheldrick, *Acta Crystallographica Section C* **2015**, *71*, 3-8.